Nonlinear Dyn (2024) 112:20549–20571
https://doi.org/10.1007/s11071-024-10098-9

RESEARCH

Exploring bifurcations in a differential-algebraic model of predator–prey interactions

Guodong Zhang · Huangyu Guo · Leimin Wang

Received: 7 February 2024 / Accepted: 26 July 2024 / Published online: 8 August 2024
© The Author(s), under exclusive licence to Springer Nature B.V. 2024

Abstract In this work, we first discuss the positive equilibrium point of the continuous predator–prey system and its stability, and we discuss the parameter conditions under which the continuous system undergoes a cusp bifurcation (Bogdanov–Takens bifurcation) of codimension two bifurcation at the positive equilibrium point. Then, we provide an insightful study of discrete predator–prey systems by the use of Euler's method, which includes square-root function responses and nonlinear prey harvesting. By synthesizing the new standard form of differential-algebraic systems, the central manifold theorem, and the bifurcation theory, we identify the specific conditions under which the system may undergo flip bifurcation and Neimark–Sacker bifurcation. In addition, codimension-two bifurcations associated with 1:2 strong resonances are analyzed by using a series of affine transformations and bifurcation theory. Through numerical simulations, we not only verify the validity and correctness of our findings, but also elucidate the frequency of trajectory bifurcations in the intervals of 2, 4, and 8 and chaotic phenomena. These findings reveal a richer and more diverse dynamic behavior of discrete differential-algebraic bioeconomic systems, which is of great theoretical and practical significance to the fields of mathematics and biology.

Keywords Bifurcation · Discrete differential-algebraic system · Stability · Chaos · Neimark–Sacker bifurcation · Bogdanov–Takens bifurcation

Mathematics Subject Classification 34D20 · 92D25

1 Introduction

The history of predator–prey interactions can be traced back to the early stages of ecology and biology. Predator–prey interactions play an important role in ecosystems and are essential for maintaining biodiversity and ecological balance. Researchers [1–5] have investigated the system stability and bifurcation analysis of continuous predator–prey systems with different functional response functions. The different functional response functions include Beddington-DeAngelis functional response, constant capture and prey group defense, among others. Researchers [6–20] focused on predator–prey systems, considered the effects of different functional response functions

Huangyu Guo and Leimin Wang have contributed equally to this work.

G. Zhang (✉) · H. Guo
School of Mathematics and Statistics, South-Central Minzu University, Wuhan 430074, China
e-mail: zgd2008@mail.scuec.edu.cn

H. Guo
e-mail: 2022110533@mail.scuec.edu.cn

L. Wang
School of Automation, China University of Geosciences, Wuhan 430074, China
e-mail: wangleimin@cug.edu.cn

and delays on the system dynamics, and revealed the complex behaviors of the system under different delay conditions through in-depth mathematical analysis. The delays include time delays under different functional response and intraspecific competition conditions, hybrid delays, and so on. Researchers [21] proposed the Laplace transform-homolunculus uptake method for analyzing the dynamic properties of fractional-order time-diffusion predator–prey models in ecology, providing a new mathematical tool for numerical simulation of ecosystems. Researchers [22] simulated the modeling of the prey refuge effect in the Leslie-Gower predator–prey system and explored the dynamics of this effect in predator–prey interactions. Researchers [23] provided an in-depth analysis of the pattern dynamics of spatially fractional-order predator–prey systems with fear factors and refugia, providing new perspectives for understanding predator–prey interactions in ecosystems in complex environments. These studies not only enrich our understanding of the dynamic complexity of predator–prey systems, but also provide theoretical and practical support for ecosystem management and species conservation. Through these studies, the dynamic behavior of predator–prey interactions under different conditions can be better understood, providing scientific basis and management strategies for coping with environmental changes and ecological disasters. However, all the above systems are continuous systems, while the life cycles or behaviors of some organisms in nature are based on discrete time units or events, rather than being continuous. For example, certain insects only appear during seasonal reproduction and their life cycle is completed in a short period of time. Therefore, the dynamic behavior of discrete systems is closer to the discrete events and biological life cycles in actual ecosystems, and its study not only contributes to an in-depth understanding of the stability and dynamic properties of ecosystems, but also provides an important theoretical basis for ecological protection and resource management. So, many researchers began to focus on discrete predator–prey systems.

In recent years, several important studies involving discrete-time predator–prey systems have emerged in academia. Zhang [24] undertook an intrusive study of discrete-time predator–prey bio-economic systems, aiming to analyze the occurrence of flip-flop bifurcations and Neimark–Sacker bifurcations within the system. The study used innovative approaches such as a new normal form for differential-algebraic systems, the central manifold theorem, and bifurcation theory. Din [25], on the other hand, explores complex dynamics and chaotic control mechanisms in discrete-time predator–prey models. By introducing the Leslie-Gower predator–prey model and proposing a discrete-time predator–prey system that partially depends on the prey, the study investigates the boundedness, existence and uniqueness of the positive equilibrium points and analyzes them using the central manifold theorem and bifurcation theory. Uddin [26] provided an in-depth study of discrete prey-predator models containing predator population capture, applying Caputo fractional order derivatives. In this paper, we study a discrete predator–prey system with a square root functional response and nonlinear prey harvesting.

Mortuja [27] examined the dynamic properties of the system in the presence of nonlinear prey harvesting:

$$\begin{cases} \frac{dx(t)}{dt} = rx\left(1-\frac{x}{k}\right) - \frac{\gamma\sqrt{x}y}{1+t_h\gamma\sqrt{x}} - \frac{qEx}{m_1E+m_2x}, \\ \frac{dy(t)}{dt} = -\upsilon y + \frac{e\gamma\sqrt{x}y}{1+t_h\gamma\sqrt{x}}. \end{cases} \tag{1}$$

In the ecological context, the variables are defined as follows: x represents the population density of prey, y stands for the population density of predators, r signifies the prey population growth rate, k denotes the environmental carrying capacity, t_h represents the average handling time of bait post-predation, e is the attrition rate, γ quantifies the predator's efficiency in searching for prey, υ represents the natural mortality rate of predators in the absence of prey, q denotes the coefficient of harvesting capacity, E stands for the harvesting effort, while m_1 and m_2 are intrinsic constants.

Simultaneously, integrating practical implications, our model also introduces algebraic equations to incorporate the economic dimension of capture activities. This new model comprehensively considers a wide range of factors related to the profitability of capture activities, providing a more holistic view of our understanding of predator–prey system dynamics by integrating ecological and economic factors. According to the economic theory of Gordon [28]: net economic return (NER) is calculated as the value obtained by subtracting total costs (TC) from total revenue (TR).

In the framework of the system (1), the expressions for Total Revenue (TR) and Total Cost (TC) are as follows:

$$TR = \frac{qEx}{m_1E + m_2x}p,$$
$$TC = \frac{qE}{m_1E + m_2x}c,$$

In the context, p symbolizes the price per unit of harvested biomass, while c denotes the cost per unit of harvest. The economic profit, represented as m, is identical to the Net Economic Revenue (NER). Hence, this correlation can be articulated by the subsequent equation:

$$NER = TR - TC = \frac{qE}{m_1E + m_2x}(px - c) = m.$$

After incorporating the biological-economic algebraic equation mentioned earlier, the depiction of system (1) can be extended into a comprehensive collection of differential-algebraic equations:

$$\begin{cases} \frac{dx(t)}{dt} = rx\left(1 - \frac{x}{k}\right) - \frac{\gamma\sqrt{x}y}{1+t_h\gamma\sqrt{x}} - \frac{qEx}{m_1E+m_2x}, \\ \frac{dy(t)}{dt} = -\upsilon y + \frac{e\gamma\sqrt{x}y}{1+t_h\gamma\sqrt{x}}, \\ 0 = \frac{qE}{m_1E+m_2x}(px - c) - m. \end{cases} \tag{2}$$

For the sake of simplicity, we let

$$F(X) = \begin{bmatrix} F_1(x, y, E) \\ F_2(x, y, E) \end{bmatrix} = \begin{bmatrix} x\left[r\left(1 - \frac{x}{k}\right) - \frac{\gamma y}{\sqrt{x}(1+t_h\gamma\sqrt{x})} - \frac{qE}{m_1E+m_2x}\right] \\ y\left[-\upsilon + \frac{e\gamma\sqrt{x}}{1+t_h\gamma\sqrt{x}}\right] \end{bmatrix},$$
$$G(X) = \frac{qE}{m_1E + m_2x}(px - c) - m,$$
$$X = [x, y, E]^T.$$

The structure of this paper is as follows: In Sect. 2, we discuss the positive equilibrium point of the continuous system and its stability, we discuss the parameter conditions under which the continuous system undergoes a cusp bifurcation (Bogdanov–Takens bifurcation) of codimension two bifurcation at the positive equilibrium point.In Sect. 3, we provide a thorough examination of the foundational properties related to system (20). In Sect. 4, we proceed to analyze the local stability of fixed points within the system. In Sect. 5, we utilizes the new normal form of discrete differential-algebraic systems [29], in conjunction with the center manifold theorem and bifurcation theory [30–32], particularly for specific parameter values, to demonstrate the occurrence of flip bifurcation and Neimark–Sacker bifurcation within system (20). In Sect. 6, we study the codimension-two bifurcations of discreted system associated with 1:2 strong resonances by using a series of affine transformations and bifurcation theory. In Sect. 7,we present numerical simulations that serve to substantiate the validity of our conclusions. In Sect. 8, we discuss the biological implications and interpretations of the findings. Finally, the paper concludes by summarizing the key findings.

The innovation points of the study are as follows:

(a) In contrast to the approach taken by Zhang [24], we incorporate nonlinearity into prey harvesting.
(b) Diverging from Din [25] and Uddin [26], our investigation involves distinct response functions.
(c) Unlike the study conducted by Guo [33], we discuss the codimensional-2 bifurcation of continuous system and undertake a transformation of the system from a continuous to a discrete framework.

2 Stability analysis and Bogdanov–Takens bifurcation of the positive fixed point

In the context of the system (2), the positive equilibrium point $X_0 = [x_0, y_0, E_0]^T$ for system (2) is given by the following equations:

$$\begin{cases} 0 = rx\left(1 - \frac{x}{k}\right) - \frac{\gamma\sqrt{x}y}{1+t_h\gamma\sqrt{x}} - \frac{qEx}{m_1E+m_2x}, \\ 0 = -\upsilon y + \frac{e\gamma\sqrt{x}y}{1+t_h\gamma\sqrt{x}}, \\ 0 = \frac{qE}{m_1E+m_2x}(px - c) - m. \end{cases}$$

The system (2) has the only one positive fixed point $X_0 = (x_0, y_0, E_0)$, where:

$$x_0 = \left(\frac{\upsilon}{\gamma(e - t_h\upsilon)}\right)^2,$$
$$y_0 = \frac{\sqrt{x_0}(1 + t_h\gamma\sqrt{x_0})}{\gamma}\left(r - \frac{r}{k}x_0 - \frac{qE_0}{m_1E_0 + m_2x_0}\right),$$
$$E_0 = \frac{mm_2x_0}{qpx_0 - qc - mm_1}.$$

It's essential to emphasize that our focus is solely on the interior equilibrium of system (2). This concentration on the interior equilibrium is warranted by its biological significance, signifying the coexistence of prey, predator, and the effort exerted on prey harvesting. Consequently, in this paper, we assume that:

$$r - \frac{r}{k}x_0 - \frac{qE_0}{m_1E_0 + m_2x_0} > 0, \quad qpx_0 - qc - mm_1 > 0$$

Following the methodology outlined in the literature [34,35], we initially consider the local parametrization

Ψ of the third equation of system (2), defined as follows:

$$[x, y, E]^T = \Psi(Y) = X_0^T + U_0 Y + V_0 h(Y), g(\Psi(Y)) = 0,$$

Here, $U_0 = \begin{bmatrix} I_2 \\ 0 \end{bmatrix}$, where $I_2 = \begin{pmatrix} 1 & 0 \\ 0 & 1 \end{pmatrix}$. Additionally, $V_0 = (0, 0, 1)^T$, $Y = (y_1, y_2)^T$, and $h : \mathbb{R}^2 \to \mathbb{R}$ is a smooth mapping. Expanding on the defined Ψ and referring to [29], we can derive:

$$D\Psi(Y) = (D_{y_1}\Psi(Y), D_{y_2}\Psi(Y)) = \begin{pmatrix} Dg(X) \\ U_0^T \end{pmatrix}^{-1} \begin{pmatrix} 0 \\ I_2 \end{pmatrix}, \tag{3}$$

For additional details regarding the local parameterization, refer to [29]. The parametric representation of system (2) can be expressed as:

$$\begin{cases} \dot{\beth}_1 = f_1(m, \Psi(m, \beth)), \\ \dot{\beth}_2 = f_2(m, \Psi(m, \beth)). \end{cases} \tag{4}$$

Now, we're looking for the Jacobian matrix of the linearization part for the system (2) when evaluated at the fixed point X_0.

To calculate the Jacobian matrix, we would need the linearization equations that define the system (2). So we can proceed with the calculation of the Jacobian matrix evaluated at the fixed point:

$$\begin{aligned} & Q_Y f(\Psi(0)) \\ &= Qf(X_0)Q\Psi(0) \\ &= \begin{pmatrix} \frac{qpx_0E_0}{(px_0-c)(m_1E_0+m_2x_0)} - \frac{r}{k}x_0 + \frac{\gamma y_0(1+2t_h\gamma\sqrt{x_0})}{2\sqrt{x_0}(1+t_h\gamma\sqrt{x_0})^2} & -\frac{\gamma\sqrt{x_0}}{1+t_h\gamma\sqrt{x_0}} \\ \frac{e\gamma y_0}{2\sqrt{x_0}(1+t_h\gamma\sqrt{x_0})^2} & 0 \end{pmatrix} \end{aligned} \tag{5}$$

Theorem 1 *Considering the positive equilibrium point X_0 in system (2):*

(i) *If $a_1^2(m) > 4a_2(m)$, the positive equilibrium point X_0 is asymptotically stable for $a_1(m) > 0$ and unstable for $a_1(m) < 0$.*

(ii) *If $a_1^2(m) < 4a_2(m)$, the positive equilibrium point X_0 acts as a sink for $a_1(m) > 0$ and a source for $a_1(m) < 0$.*

Proof The characteristic equation of matrix Q reveals:

$$\lambda^2 + a_1(m)\lambda + a_2(m) = 0 \tag{6}$$

where

$$a_1(m) = \frac{r}{k}x_0 - \frac{qpx_0E_0}{(px_0 - c)(m_1E_0 + m_2x_0)} - \frac{\gamma y_0(1 + 2t_h\gamma\sqrt{x_0})}{2\sqrt{x_0}\left(1 + t_h\gamma\sqrt{x_0}\right)^2}$$

and,

$$a_2(m) = \frac{e\gamma^2 y_0}{2\left(1 + t_h\gamma\sqrt{x_0}\right)^3}$$

We denote Δ by

$$\begin{aligned} \Delta = & \left(\frac{r}{k}x_0 - \frac{qpx_0E_0}{(px_0 - c)(m_1E_0 + m_2x_0)} - \frac{\gamma y_0(1 + 2t_h\gamma\sqrt{x_0})}{2\sqrt{x_0}\left(1 + t_h\gamma\sqrt{x_0}\right)^2}\right)^2 \\ & - \frac{e\gamma^2 y_0}{2\left(1 + t_h\gamma\sqrt{x}\right)^3} \\ = & a_1^2(m) - 4a_2(m) \end{aligned}$$

Clearly, when $a_1^2(m) > 4a_2(m)$ and $a_1(m) > 0$, the roots of the Eq. (2) all have negative real parts. Conversely, when $a_1^2(m) > 4a_2(m)$ and $a_1(m) < 0$, the roots of the Eq. (2) all have positive real parts. Therefore, the first part has been proved, the second part can likewise be proved. □

Then, it is proved that the unique positive equilibrium point of system is the cusp of codimensional-2. Then, we discuss Bogdanov-Takens bifurcation (B-T bifurcation). If $f(x, y, E) = 0$ and $f'(x, y, E) = 0$ hold simultaneously, then there is a pair of mutually coupled positive equilibrium points, generating a degenerate equilibrium point, denoted as $X_0(x_0, y_0, E_0)$ If $det(Q|X_0) = 0$and $tr(Q|X_0) = 0$, then the Jacobian matrix at Q has a pair of double roots 0, so X_0 will be a sharp point.

To discern the properties of Hopf bifurcation in system (2), we follow the approach outlined in [36,37]. It requires transforming system (2) into the following form:

$$\begin{cases} \dfrac{\mathrm{d}\beth_1}{\mathrm{d}t} = a_1\beth_1 + b_1\beth_1 + p_{11}\beth_1^2 + p_{12}\beth_1\beth_2 + p_{22}\beth_2^2 + \mathrm{O}(\|\beth\|^3), \\ \dfrac{\mathrm{d}\beth_2}{\mathrm{d}t} = c_1\beth_1 + d_1\beth_2 + q_{11}\beth_1^2 + q_{12}\beth_1\beth_2 + q_{22}\beth_2^2 + \mathrm{O}(\|\beth\|^3) \end{cases} \tag{7}$$

where

$$
\begin{aligned}
a_1 =& \frac{qpx_0E_0}{(px_0-c)(m_1E_0+m_2x_0)} - \frac{r}{k}x_0 \\
&+ \frac{\gamma y_0(1+2t_h\gamma\sqrt{x_0})}{2\sqrt{x_0}\left(1+t_h\gamma\sqrt{x_0}\right)^2}, \\
b_1 =& -\frac{\gamma\sqrt{x_0}}{1+t_h\gamma\sqrt{x_0}}, \\
c_1 =& \frac{e\gamma y_0}{2\sqrt{x_0}\left(1+t_h\gamma\sqrt{x_0}\right)^2}, \\
d_1 =& 0, \\
p_{11} =& \frac{\gamma y_0(1+3t_h\gamma\sqrt{x_0})}{4x_0^{\frac{3}{2}}(1+t_h\gamma\sqrt{x_0})^3} - \frac{2r}{k} + \frac{2E_0^2m_1m_2q}{(m_1E_0+m_2x_0)^3} \\
&- \frac{2E_0q\left(m_1pE_0+m_2c\right)\left(cm_1E_0+m_2p^2x_0\right)}{(px_0-c)^2(m_1E_0+m_2x_0)^3} \\
p_{12} =& -\frac{\gamma}{2\sqrt{x_0}(1+t_h\gamma\sqrt{x_0})}, \\
p_{22} =& 0, \\
q_{11} =& \frac{\gamma ey_0(1+3t_h\gamma\sqrt{x_0})}{8x_0^{\frac{3}{2}}(1+t_h\gamma\sqrt{x_0})^3}, \\
q_{12} =& \frac{e\gamma}{2\sqrt{x_0}(1+t_h\gamma\sqrt{x_0})}, \\
q_{22} =& 0.
\end{aligned}
$$

and

$$a_1+d_1=0, \quad a_1d_1-b_1c_1=0.$$

Translating

$$\ell_1=\beth_1, \quad \ell_2=a_1\beth_1+b_1\beth_2$$

Then system (7) can be reduced to

$$
\begin{cases}
\frac{\mathrm{d}\ell_1}{\mathrm{d}t} = \ell_2 + a_{11}\ell_1^2 + a_{12}\ell_1\ell_2 + \mathrm{O}(\|\ \ell\ \|^3), \\
\frac{\mathrm{d}\ell_2}{\mathrm{d}t} = \beta_{11}\ell_1^2 + \beta_{12}\ell_1\ell_2 + \mathrm{O}(\|\ \ell\ \|^3),
\end{cases} \tag{8}
$$

where

$$a_{11}=-\frac{p_{12}}{b_1}+p_{11}, \quad a_{12}=\frac{p_{12}}{b_1},$$

$$\beta_{11}=b_1q_{11}+a_1\left(p_{11}-q_{12}\right)-\frac{a_1^2p_{12}}{b_1},$$

$$\beta_{12}=\frac{a_1^2p_{12}}{b_1}+q_{12}.$$

There exists a C^∞ as follows

$$
\begin{cases}
\iota_1 = \ell_1 - \frac{1}{2}\cdot\frac{p_{12}}{b_1}\ell_1^2, \\
\iota_2 = \ell_2 + \left(p_{11}-\frac{a_1p_{12}}{b_1}\right)\ell_1^2.
\end{cases}
$$

So the system (8) is reduced to

$$
\begin{cases}
\frac{\mathrm{d}\iota_1}{\mathrm{d}t} = \iota_2 + \mathrm{O}(\|\ \iota\ \|^3), \\
\frac{\mathrm{d}\iota_2}{\mathrm{d}t} = \rho_1\iota_1^2 + \rho_2\iota_1\iota_2 + \mathrm{O}(\|\ \iota\ \|^3),
\end{cases}
$$

where

$$\rho_1=\beta_{11}, \quad \rho_2=-\frac{a_1}{b_1}p_{12}+2p_{11}+q_{12}.$$

Noticing that $_{\rho_1\rho_1}\neq 0$ (non-degenerate condition), hence the immovable point X_0 is a cusp of cosimplicial dimension-2. Thus, the following theorem is obtained.

Theorem 2 *System (2) has a cusp of dimension-2 at the degenerate equilibrium X_0.*

Theorem 3 *If γ, e is chosen as the bifurcation parameter, then the system (2) undergoes a B-T bifurcation in a small neighborhood of X_0.*

Proof Considering the disturbed system

$$
\begin{cases}
\dot{x} = x\left[r\left(1-\frac{x}{k}\right) - \frac{(\gamma+\jmath_1)y}{\sqrt{x}(1+t_h(\gamma+\jmath_1)\sqrt{x})} - \frac{qE}{m_1E+m_2x}\right], \\
\dot{y} = y\left[-\upsilon + \frac{(e+\jmath_2)(\gamma+\jmath_1)\sqrt{x}}{1+t_h(\gamma+\jmath_1)\sqrt{x}}\right], \\
0 = \frac{qE}{m_1E+m_2x}(px-c)-m.
\end{cases} \tag{9}
$$

where $(\jmath_1, \jmath_2)$ is the parameter vector in a small neighborhood of $(0, 0)$. According to the above transformation, the system becomes:

$$
\begin{cases}
\frac{\mathrm{d}\beth_1}{\mathrm{d}t} = p_0(\jmath) + a_2(\jmath)\beth_1 + b_2(\jmath)\beth_2 + p_1'(\jmath)\beth_1^2 \\
\quad + p_2'(\jmath)\beth_1\beth_2 + p_2'(\jmath)\beth_2^2 + \mathrm{O}(\|\ x\ \|^3), \\
\frac{\mathrm{d}\beth_2}{\mathrm{d}t} = q_0(\jmath) + c_2(\jmath)\beth_1 + d_2(\jmath)\beth_2 + q_{11}'(\jmath)\beth_1^2 \\
\quad + q_2'(\jmath)\beth_1\beth_2 + q_2'(\jmath)\beth_2^2 + O(\|\ x\ \|^3),
\end{cases}
$$

where

$$
\begin{aligned}
p_0(\jmath) =& -\jmath_1\sqrt{x_0}y_0,\\
q_0(\jmath) =& \jmath_2\sqrt{x_0}y_0,\\
a_2(\jmath) =& \frac{qpx_0E_0}{(px_0-c)\,(m_1E_0+m_2x_0)} - \frac{r}{k}x_0\\
&+\frac{(\gamma+\jmath_1)y_0(1+2t_h(\gamma+\jmath_1)\sqrt{x_0})}{2\sqrt{x_0}\left(1+t_h(\gamma+\jmath_1)\sqrt{x_0}\right)^2},\\
b_2(\jmath) =& -\frac{(\gamma+\jmath_1)\sqrt{x_0}}{1+t_h(\gamma+\jmath_1)\sqrt{x_0}},\\
c_2(\jmath) =& \frac{(e+\jmath_2)(\gamma+\jmath_1)y_0}{2\sqrt{x_0}\left(1+t_h(\gamma+\jmath_1)\sqrt{x_0}\right)^2},\\
d_2(\jmath) =& 0,\\
p'_{11}(\jmath) =& \frac{(\gamma+\jmath_1)y_0(1+3t_h(\gamma+\jmath_1)\sqrt{x_0})}{4x_0^{\frac{3}{2}}(1+t_h(\gamma+\jmath_1)\sqrt{x_0})^3}\\
&-\frac{2r}{k}+\frac{2E_0^2m_1m_2q}{(m_1E_0+m_2x_0)^3}\\
&-\frac{2E_0q\,(m_1pE_0+m_2c)\left(cm_1E_0+m_2p^2x_0\right)}{(px_0-c)^2\,(m_1E_0+m_2x_0)^3}\\
p'_{12}(\jmath) =& -\frac{(\gamma+\jmath_1)}{2\sqrt{x_0}(1+t_h(\gamma+\jmath_1)\sqrt{x_0})},\\
p'_{22}(\jmath) =& 0,\\
q'_{11}(\jmath) =& \frac{(\gamma+\jmath_1)ey_0(1+3t_h(\gamma+\jmath_1)\sqrt{x_0})}{8x_0^{\frac{3}{2}}(1+t_h(\gamma+\jmath_1)\sqrt{x_0})^3},\\
q'_{12}(\jmath) =& \frac{(e+\jmath_2)(\gamma+\jmath_1)}{2\sqrt{x_0}(1+t_h(\gamma+\jmath_1)\sqrt{x_0})},\\
q'_{22}(\jmath) =& 0.
\end{aligned}
$$

Translating

$$\ell_1 = \lrcorner_1\,,\quad \ell_2 = a_2\lrcorner_1 + b_2\lrcorner_2$$

And we get

$$
\begin{cases}
\frac{\mathrm{d}\ell_1}{\mathrm{d}t} = p_0(\jmath)+\ell_2+a'_{11}(\jmath)\,\ell_1^2\\
\quad +a'_{12}(\jmath)\,\ell_1\ell_2+\mathrm{O}\left(\|\ell\|^3\right),\\
\frac{\mathrm{d}\ell_2}{\mathrm{d}t} = q'_0(\jmath)+c_3(\jmath)\,\ell_1+d_3(\jmath)\,\ell_2+\beta_{11}(\jmath)\,y_1^2\\
\quad +\beta_{12}(\jmath)\,\ell_1\ell_2+\mathrm{O}\left(\|\ell\|^3\right),
\end{cases}
\tag{10}
$$

where

$$
\begin{aligned}
q'_0(\jmath) =& p_0a_2+q_0b_2,\\
& c_3 = b_2c_2-a_2d_2,\quad d_3 = a_2+d_2,\\
a'_{11} =& p'_{11}-\frac{a_2p'_{12}}{b_2},\quad a'_{12}=\frac{p'_{12}}{b_2},\\
& \beta'_{12}=\frac{a_2p'_{12}}{b_2}+q'_{12},\\
\beta'_{11} =& b_2q'_{11}+a_2(p'_{11}-q'_{12})-\frac{a_2^2p'_{12}}{b_2}.
\end{aligned}
$$

The functions $q'_0(\jmath), a_i, \beta_i$ are smooth functions on $\jmath$. Noting that $q'_0(\jmath^*) = c_3(\jmath^*) = d_3(\jmath^*) = 0$, considering the following transformations:

$$
\begin{aligned}
\imath_1 =& \ell_1,\ \imath_2 = p_0(\jmath)+\ell_2+\alpha'_{11}(\jmath)\ell_1^2\\
&+\alpha'_{12}(\jmath)\ell_1\ell_2+\mathcal{O}(\|\ell\|^3),
\end{aligned}
$$

So the system (10) is reduced to

$$
\begin{cases}
\frac{\mathrm{d}\imath_1}{\mathrm{d}t} = \imath_2\,,\\
\frac{\mathrm{d}\imath_2}{\mathrm{d}t} = k_{00}(\jmath)+k_{10}(\jmath)\imath_1+k_{01}(\jmath)\imath_2+k_{20}(\jmath)\imath_1^2\\
\quad +k_{11}(\jmath)\imath_1\imath_2+k_{02}(\jmath)\imath_2^2+\mathrm{O}(\|\imath\|^3)\,.
\end{cases}
\tag{11}
$$

And

$$
\begin{aligned}
k_{00}(0) =& 0,\quad g_{10}(0)=0,\quad g_{01}(0)=0,\\
\imath =& (\imath_1,\imath_2)\,,\\
k_{00}(\jmath) =& q'_0(\jmath)-p_0(\jmath)\,d_3(\jmath)+\cdots,\\
k_{10}(\jmath) =& c_3(\jmath)+\alpha'_{12}(\jmath)\,q'_0(\jmath)-\beta'_{12}(\jmath)\,p_0(\jmath)+\cdots,\\
k_{01}(\jmath) =& d_3(\jmath)-\alpha'_{12}(\jmath)\,p_0(\jmath)\,,\\
k_{20}(\jmath) =& \beta'_{11}(\jmath)-\alpha'_{11}(\jmath)\,d_3(\jmath)+c_3(\jmath)\,a'_{12}(\jmath)+\cdots,\\
k_{11}(\jmath) =& \beta'_{12}(\jmath)+2\alpha'_{11}(\jmath)-\alpha'_{12}(\jmath)\,d_3(\jmath)+\cdots,\\
k_{02}(\jmath) =& \alpha'_{12}(\jmath)+\cdots,
\end{aligned}
$$

Correspondingly

$$
\begin{aligned}
&k_{00}\left(\jmath^*\right)=0, k_{10}\left(\jmath^*\right)=0,\\
&k_{01}\left(\jmath^*\right)=0,\quad k_{20}\left(\jmath^*\right)=\beta'_{11}\left(\jmath^*\right),\\
&k_{02}\left(\jmath^*\right)=\alpha'_{11}\left(\jmath^*\right),\\
&k_{11}\left(\jmath^*\right)=\beta'_{12}\left(\jmath^*\right)+2\alpha'_{11}\left(\jmath^*\right).
\end{aligned}
$$

Further system (11) is written in the following form:

$$
\begin{cases}
\frac{\mathrm{d}\imath_1}{\mathrm{d}t} = \imath_2\,,\\
\frac{\mathrm{d}\imath_2}{\mathrm{d}t} = (k_{00}(\jmath)+k_{10}(\jmath)\imath_1+k_{20}(\jmath)\imath_1^2\\
+\mathrm{O}(\|\imath\|^3))+(k_{01}(\jmath)+(g_{11}(\jmath)\imath_1+\mathrm{O}(\|\imath\|^2)))\imath_2\\
+(k_{02}(\jmath)+\mathrm{O}(\|\imath\|))\imath_2^2\\
=\urcorner(\imath_1,\jmath)+\jmath(\imath_1,\jmath)\imath_2+\eth(\imath,\jmath)\imath_2^2,
\end{cases}
\tag{12}
$$

where $\urcorner, \jmath, \eth$ is a smooth function,and satisfies the following conditions

$$
\begin{aligned}
&\urcorner(0,\jmath^*)=k_{00}(\jmath^*)=0,\quad \jmath(0,\jmath^*)=k_{01}(\jmath^*)=0,\\
&\left.\frac{\partial\urcorner}{\partial\imath_1}\right|_{(0,\jmath^*)}=k_{10}\left(\jmath^*\right)=0,\\
&\left.\frac{\partial^2\urcorner}{\partial\imath_1^2}\right|_{(0,\jmath^*)}=k_{20}(\jmath^*)=\beta'_{11}(\jmath^*)=\rho_1\neq 0\,,\\
&\left.\frac{\partial\,\jmath}{\partial\imath_1}\right|_{(0,\jmath^*)}=k_{11}(\jmath^*)=\beta'_{11}(\jmath^*)+2\alpha'_{11}(\jmath^*)=\rho_2\neq 0.
\end{aligned}
$$

Due to

$$\urcorner(0,\jmath^*)=0\,,\quad \left.\frac{\partial\,\jmath}{\partial\imath_1}\right|_{(0,\jmath^*)}=\rho_2\neq 0\,,$$

By the implicit function theorem, there exists a C^∞ function ι_1 (defined in a small neighborhood of $\jmath = \jmath^*$) such that $\Re(\jmath^*) = 0$, $\mathfrak{z}(\Re, \jmath) = 0$, for any For any $\jmath \in \mathbb{N}(\jmath^*)$, the following polar transformations are used to eliminate the right-hand side term of the second equation of system (12).

Let $\iota_1 = \urcorner_1 + \Re(\jmath)$, $\iota_2 = \urcorner_2$, then system (12) can be transformed into

$$\begin{cases} \frac{\mathrm{d}\urcorner_1}{\mathrm{d}t} = \urcorner_2 , \\ \frac{\mathrm{d}\urcorner_2}{\mathrm{d}t} = (h_{00}(\jmath) + h_{10}(\jmath)\urcorner_1 + h_{20}(\jmath)\urcorner_1^2 \\ +O(\| \urcorner \|^3)) + (h_{01}(\jmath) \\ +(h_{11}(\jmath)\urcorner_1 + O(\| \urcorner \|^2)))\urcorner_2 \\ +(h_{02}(\jmath) + \mathrm{O}(\| \urcorner \|))u_2^2 \\ = \overline{\urcorner}(\urcorner_1, \jmath) + \bar{\mathfrak{z}}(\urcorner_1, \jmath)\urcorner_2 + \bar{\eth}(\urcorner, \jmath)\urcorner_2^2, \end{cases} \tag{13}$$

where

$$h_{00} = k_{00} + k_{10}\Re + \cdots , \quad h_{10} = k_{10} + 2k_{20}\Re + \cdots ,$$
$$h_{01} = k_{01} + k_{11}\Re + \cdots , \quad h_{11} = k_{11} + \cdots ,$$
$$h_{02} = k_{02} + \cdots , \quad h_{20} = k_{20} + \cdots , \quad \urcorner = (\urcorner_1, \urcorner_2).$$

The coefficients of the $\urcorner$, term on the right hand side of the second equality of Eq. (13) can be determined by the following equation

$$\begin{aligned} h_{01} &= \bar{\mathfrak{z}}(0, \jmath) = g_{01} + g_{11}\Re + \mathrm{O}(\| \Re \|^2) \\ &= [d_2 - a'_{12}p_0 + \cdots] \\ &\quad +[\beta'_{12} + 2\alpha'_{11} - \alpha'_{12}d_2 + \cdots]\Re, \end{aligned}$$

Then, we can get

$$h_{01}(0, \jmath) = k_{01}(\jmath^*) = 0, \quad \left.\frac{\partial h_{01}}{\partial \Re}\right|_{(0,\jmath^*)}$$
$$= \beta_{12}(\jmath^*) + 2\alpha'_{11}(\jmath^*) = \rho_2 \neq 0,$$

Let $\jmath \in \mathcal{N}(\jmath^*), \Re(\jmath) \in \mathcal{M}$, then $\Re(\jmath) \in$ a neighborhood of M can be approximated as $\Re(\jmath) \approx -k_{01}(\jmath)/\rho_2$, so system (13) can be reduced to

$$\begin{cases} \frac{\mathrm{d}\urcorner_1}{\mathrm{d}t} = \urcorner_2 , \\ \frac{\mathrm{d}\urcorner_2}{\mathrm{d}t} = h_{00}(\jmath) + h_{10}(\jmath)\urcorner_1 + h_{20}(\jmath)\urcorner_1^2 \\ +h_{11}(\jmath)\urcorner_1\urcorner_2 + h_{02}(\jmath)\urcorner_2^2 + (0(\| \urcorner \|^3) . \end{cases} \tag{14}$$

Introducing the new time scalar $\mathrm{d}t = (1 + \psi u_1)\mathrm{d}\tau$, where $\psi = \psi(\jmath)$ is the smooth function, transforms equation (14) into

$$\begin{cases} \frac{\mathrm{d}\urcorner_1}{\mathrm{d}\tau} = \urcorner_2 (1 + \psi\urcorner_1) , \\ \frac{\mathrm{d}\urcorner_2}{\mathrm{d}\tau} = h_{00} + (h_{10} + h_{00}\psi)\urcorner_1 + (h_{20} + h_{10}\psi)\urcorner_1^2 \\ +h_{11}\urcorner_1\urcorner_2 + h_{02}\urcorner_2^2 + \mathrm{O}(\| \urcorner \|^3). \end{cases} \tag{15}$$

Assuming $\mathfrak{z}_1 = \urcorner_1$, $\mathfrak{z}_2 = \urcorner_2(1 + \psi\urcorner_1)$, we have that

$$\begin{cases} \frac{\mathrm{d}\ \mathfrak{z}_1}{\mathrm{d}\tau} = \mathfrak{z}_2 , \\ \frac{\mathrm{d}\ \mathfrak{z}_2}{\mathrm{d}\tau} = l_{00}(\jmath) + l_{10}(\jmath)\ \mathfrak{z}_1 + l_{20}(\jmath)\ \mathfrak{z}_1^2 \\ +l_{11}(\jmath)\ \mathfrak{z}_1\mathfrak{z}_2 + l_{02}(\jmath)\ \mathfrak{z}_2^2 + \mathrm{O}(\| \mathfrak{z} \|^3) , \end{cases} \tag{16}$$

where

$$\begin{aligned} l_{00}(\jmath) &= h_{00} , \quad l_{20}(\jmath) \\ &= h_{20} + 2h_{00}\psi(\jmath) + h_{00}\psi^2(\jmath) , \\ l_{11}(\jmath) &= h_{11} , \quad l_{02}(\jmath) \\ &= h_{02} + \psi(\jmath) , \quad l_{10}(\jmath) = h_{10} + 2h_{00}\psi(\jmath) . \end{aligned}$$

Let $\psi(\jmath) = -h_{02}(\jmath)$, to eliminate the $\mathfrak{z}_2^2$ term, then

$$\begin{cases} \frac{\mathrm{d}\ \mathfrak{z}_1}{\mathrm{d}\tau} = \mathfrak{z}_2 , \\ \frac{\mathrm{d}\ \mathfrak{z}_2}{\mathrm{d}\tau} = \beta_1(\jmath) + \beta_2(\jmath)\ \mathfrak{z}_1 + \eta(\jmath)\ \mathfrak{z}_1^2 \\ +\zeta(\jmath)\ \mathfrak{z}_1\mathfrak{z}_2 + \mathrm{O}(\| \mathfrak{z} \|^3) , \end{cases} \tag{17}$$

where

$$\mathfrak{z} = (\ \mathfrak{z}_1\ ,\ \mathfrak{z}_2\ ) , \quad \beta_2(\jmath) = h_{10}(\jmath) - 2h_{00}(\jmath)h_{02}(\jmath) ,$$
$$\beta_1(\jmath) = h_{00}(\jmath), \quad \zeta(\jmath) = h_{11}(\jmath) \neq 0, \quad h_{00}(\jmath) \neq 0 ,$$
$$\eta(\jmath) = h_{20}(\jmath) - 2h_{10}(\jmath)h_{02}(\jmath) + h_{02}^2(\jmath).$$

Introducing the new time variable $t = \left|\frac{\eta(\jmath)}{\zeta(\jmath)}\right| \tau$ and the new variables $\xi_1 = \frac{\eta(\jmath)}{\zeta^2(\jmath)}\ \mathfrak{z}_1$, $\xi_2 = \frac{\eta^2(\jmath)}{\zeta^3(\jmath)}\ \mathfrak{z}_2$, then

$$s = sign\ \frac{\eta(\jmath)}{\zeta(\jmath)} = sign\ \frac{\eta^*(\jmath)}{\zeta^*(\jmath)}$$
$$= \frac{\rho_2}{k_{20}(\jmath^*)} = \pm 1$$

Thus Eq. (17) can be changed to

$$\begin{cases} \frac{\mathrm{d}\xi_1}{\mathrm{d}\tau} = \xi_2 , \\ \frac{\mathrm{d}\xi_2}{\mathrm{d}\tau} = \Bbbk_1 + \Bbbk_2\xi_1 + \xi_1^2 + s\xi_1\xi_2 + \mathrm{O}(\| \xi \|^3) , \end{cases} \tag{18}$$

where

$$\Bbbk_1(\jmath) = \frac{\eta(\jmath)}{\zeta^2(\jmath)}\beta_1(\jmath) , \quad \Bbbk_2(\jmath) = \frac{\eta(\jmath)}{\zeta^2(\jmath)}\beta_2(\jmath) ,$$

Then Eq. (18) is locally topologically equivalent (for arbitrarily small $\|_\Bbbk\|$) at the origin to the following equation

$$\begin{cases} \frac{\mathrm{d}\xi_1}{\mathrm{d}\tau} = \xi_2 , \\ \frac{\mathrm{d}\xi_2}{\mathrm{d}\tau} = \Bbbk_1 + \Bbbk_2\xi_1 + \xi_1^2 + s\ \xi_1\xi_2 . \end{cases} \tag{19}$$

Then, we get the general paradigm for the B-T bifurcation of the system (2),

$$\operatorname{rank}\left(\frac{\partial\left(\mathbb{k}_1,\mathbb{k}_2\right)}{\partial J}\right)=2,\quad J=\begin{vmatrix}\frac{\partial \urcorner_1}{\partial J_2} & \frac{\partial \urcorner_1}{\partial J_1}\\ \frac{\partial \urcorner_2}{\partial J_2} & \frac{\partial \urcorner_2}{\partial J_1}\end{vmatrix}\neq 0.$$

□

Remark 1 The Bogdanov–Takens Point is characterized by the coexistence of a stable limit cycle and a saddle-focus equilibrium. Near this point, the phase space exhibits complex dynamics due to the interaction between these two coexisting structures. A homoclinic orbit is a periodic orbit that is asymptotic, in both forward and backward time, to a saddle equilibrium point. Near the Bogdanov–Takens Point, a curve of homoclinic orbits emerges due to the presence of the saddle-focus equilibrium. These orbits play a crucial role in shaping the global dynamics of the system.

3 Fundamental characteristics of discrete system (2)

Discretizing predator–prey systems simplifies the model analysis process, enhances the convenience of numerical simulations, and offers strong adaptability and improved mathematical descriptions. Consequently, we proceed to discretize the aforementioned system.Utilizing the forward Euler method on system (2), we devise an innovative discrete-time biological-economic system, characterized by a set of discrete-time differential-algebraic equations outlined as follows:

$$\begin{cases} x\to & x+\delta x[r\left(1-\frac{x}{k}\right)-\frac{\gamma y}{\sqrt{x}(1+t_h\gamma\sqrt{x})}-\frac{qE}{m_1E+m_2x}],\\ y\to & y+\delta y[-\upsilon+\frac{e\gamma\sqrt{x}}{1+t_h\gamma\sqrt{x}}],\\ 0= & \frac{qE}{m_1E+m_2x}(px-c)-m. \end{cases} \tag{20}$$

For simplicity, let

$$\begin{aligned} f(X)&=\begin{bmatrix} f_1(x,y,E)\\ f_2(x,y,E)\end{bmatrix}\\ &=\begin{bmatrix} x+\delta x[r\left(1-\frac{x}{k}\right)-\frac{\gamma y}{\sqrt{x}(1+t_h\gamma\sqrt{x})}-\frac{qE}{m_1E+m_2x}]\\ y+\delta y[-\upsilon+\frac{e\gamma\sqrt{x}}{1+t_h\gamma\sqrt{x}}]\end{bmatrix},\\ g(X)&=\frac{qE}{m_1E+m_2x}(px-c)-m,\\ X&=[x,y,E]^T. \end{aligned}$$

Given that the set Ξ_0 is defined as $\{X=(x,y,E)\mid x>0,y>0,E>0\}$, and given its practical applications in the field of bioeconomics, this paper focuses mainly on the study of the system (20) within the domain Ξ_0. Our goal is to determine the conditions under which the solution of the system (20) remains positive and bounded in this domain.

Lemma 1 *Assuming that the condition $m>0$ is satisfied, we can say with certainty that for system (20), every possible solution $(x,\ y,\ E)$ with initial values $x_1>0,\ y_1>0$, and $E_1>0$ is not only positive but also constrained by the specified domain Ξ_0.*

Proof The formulation of system (20) can be rephrased as follows:

$$\begin{cases} x_{n+1}=x_n+\delta x_n\\ \left[r\left(1-\frac{x_n}{k}\right)-\frac{\gamma y_n}{\sqrt{x_n}(1+t_h\gamma\sqrt{x_n})}-\frac{qE_n}{m_1E_n+m_2x_n}\right],\\ y_{n+1}=y_n+\delta y_n\left[-\upsilon+\frac{e\gamma\sqrt{x_n}}{1+t_h\gamma\sqrt{x_n}}\right],\\ 0=\frac{qE_n}{m_1E_n+m_2x_n}(px_n-c)-m, \end{cases} \tag{21}$$

that is

$$\begin{cases} x_{n+1}=x_n\\ \left(1+\delta r\left(1-\frac{x_n}{k}\right)-\frac{\delta\gamma y_n}{\sqrt{x_n}(1+t_h\gamma\sqrt{x_n})}-\frac{\delta qE_n}{m_1E_n+m_2x_n}\right),\\ y_{n+1}=y_n\left(1-\delta\upsilon+\frac{\delta e\gamma\sqrt{x_n}}{1+t_h\gamma\sqrt{x_n}}\right),\\ 0=\frac{qE_n}{m_1E_n+m_2x_n}(px_n-c)-m, \end{cases} \tag{22}$$

from a biological perspective, let x_n, y_n, and E_n represent prey density, predator density, and harvest effort, respectively. Considering system (19), we can deduce that $\sup_{\forall n\in\mathbb{N}}x_n\leqslant\frac{k+k\delta r}{\delta r}$, $\sup_{\forall n\in\mathbb{N}}y_n\leqslant\frac{(1+\delta r)^2(1+t_h\gamma)}{\gamma\delta^2 r}$, and $\sup_{\forall n\in\mathbb{N}}E_n\leqslant\frac{(1+\delta r)^2m_2k}{(q\delta-m_1-m_1\delta r)r\delta}$. In the practical context of biological economics, it is understood that prey density $x_n>0$, predator density $y_n>0$, and harvest effort $E_n>0$ for all $n\in\mathbb{N}$, thus completing the proof. □

Moving forward, our goal is to determine all possible fixed points of system (20). The fixed points $X_0=(x_0,y_0,E_0)$ of the mapping (20) satisfy the following system of equations:

$$\begin{cases} x=x+\delta x\left[r\left(1-\frac{x}{k}\right)-\frac{\gamma y}{\sqrt{x}(1+t_h\gamma\sqrt{x})}-\frac{qE}{m_1E+m_2x}\right],\\ y=y+\delta y\left[-\upsilon+\frac{e\gamma\sqrt{x}}{1+t_h\gamma\sqrt{x}}\right],\\ 0=\frac{qE}{m_1E+m_2x}(px-c)-m, \end{cases} \tag{23}$$

Theorem 4 *The system (20) also has the only one positive fixed point $X_0=(x_0,y_0,E_0)$.*

Remark 2 The proof of Lemma 1 mainly depends on a biological viewpoint. In fact, referring to [38], it becomes apparent that Lemma 1 remains valid for system (2).

Remark 3 The main difference between discrete ecosystems and continuous ecosystems lies in the spatial and temporal structure between their components. Ecosystems are usually extremely complex, involving a large number of species, interactions, and environmental factors. Through discretization, complex continuous systems can be decomposed into discrete units or processes, making understanding and modeling of the system more feasible. This simplification can help researchers focus on specific ecological units or processes and better understand their behavior.

4 Stability analysis of the positive fixed point

In this section, we focus on analyzing the local stability of the positive fixed point $X_0 = (x_0, y_0, E_0)$. Derived from (20), we obtain $Dg(x_0, y_0, E_0) = (\frac{qE(pm_1E+m_2c)}{(m_1E+m_2x)^2}, 0, \frac{(px-c)m_2x}{(m_1E+m_2x)^2})$, and it is observed that the rank of $Dg(x_0, y_0, E_0)$ is 1.

For any point (x, y, E) in an open neighborhood $B_1(x_0, y_0, E_0)$, the dynamical system (20) can be effectively reduced to the following form:

$$Y \to f(\Psi(Y)), \quad Y = (y_1, y_2), \quad Y \in A \subset \mathbb{R}^2, \quad (24)$$

where A is a subset of $\mathbb{R}^2$ defined as $A = \psi^{-1}(B_1(x_0, y_0, E_0))$ with the property that the point $(0, 0)$ is an element of A. $B_1(x_0, y_0, E_0)$ represents an open neighborhood of the point (x_0, y_0, E_0) in the three-dimensional space.

Now, we're looking for the Jacobian matrix of the linearization part for the system (8) when evaluated at the fixed point $Y_0 = (0, 0)$.

To calculate the Jacobian matrix, we would need the linearization equations that define the system (24). So we can proceed with the calculation of the Jacobian matrix evaluated at the fixed point:

$$\begin{aligned} &D_Y f(\Psi(0)) \\ &= Df(X_0)D\Psi(0) \\ &= \begin{pmatrix} 1 + \frac{\delta q p x_0 E_0}{(px_0-c)(m_1E_0+m_2x_0)} - \frac{\delta r}{k}x_0 + \frac{\delta\gamma y_0(1+2t_h\gamma\sqrt{x_0})}{2\sqrt{x_0}(1+t_h\gamma\sqrt{x_0})^2} & -\frac{\delta\gamma\sqrt{x_0}}{1+t_h\gamma\sqrt{x_0}} \\ \frac{\delta e\gamma y_0}{2\sqrt{x_0}(1+t_h\gamma\sqrt{x_0})^2} & 1 \end{pmatrix} \end{aligned} \quad (25)$$

Starting from Eq. (25), it is straightforward to derive the characteristic equation for the Jacobian matrix $D_Y f(\Psi(0))$. This characteristic equation can be expressed as follows:

$$\lambda^2 - (2 + \aleph_1\delta)\lambda + (1 + \aleph_1\delta + \aleph_2\delta^2) = 0, \quad (26)$$

where

$$\begin{aligned} \aleph_1 &= \frac{qpx_0E_0}{(px_0 - c)(m_1E_0 + m_2x_0)} - \frac{r}{k}x_0 \\ &\quad + \frac{\gamma y_0(1 + 2t_h\gamma\sqrt{x_0})}{2\sqrt{x_0}\left(1 + t_h\gamma\sqrt{x_0}\right)^2}, \\ \aleph_2 &= \frac{e\gamma^2 y_0}{2(1 + t_h\gamma\sqrt{x_0})^3}. \end{aligned}$$

Now, consider λ_1 and λ_2 as two eigenvalues of the fixed point X_0. Let's explore alternative phrasing and expand upon the definitions of different topological types for a fixed point X_0: a fixed point X_0 is termed a sink and is locally stable if both eigenvalues λ_1 and λ_2 have magnitudes less than 1. Conversely, if both eigenvalues have magnitudes greater than 1, the fixed point X_0 is termed a source and is locally unstable. If one eigenvalue has a magnitude greater than 1 while the other has a magnitude less than 1 (or vice versa), X_0 is referred to as a saddle point. X_0 is labeled non-hyperbolic if either of the eigenvalues has a magnitude of exactly 1.

Let $\Gamma(\lambda) = \lambda^2 - (2 + \aleph_1\delta)\lambda + (1 + \aleph_1\delta + \aleph_2\delta^2)$, then we have

$$\Gamma(1) = \aleph_2\delta^2, \quad \Gamma(-1) = 4 + 2\aleph_1\delta + \aleph_2\delta^2. \quad (27)$$

Using Eq. (27) and referring to Lemma 2 in Liu [39], we can establish Theorem 5 concerning the local stability of the positive fixed points in system (20).

Theorem 5 *Let X_0 be the positive fixed point of (20), with $\aleph_2 > 0$, then:*

(a) *X_0 behaves as a sink under either of the following conditions:*

(a1) *When $-2\sqrt{\aleph_2} \leqslant \aleph_1 < 0$ and $0 < \delta < -\frac{\aleph_1}{\aleph_2}$.*

(a2) *When* $\aleph_1 < -2\sqrt{\aleph_2}$ *and* $0 < \delta < \frac{-\aleph_1-\sqrt{\aleph_1^2-4\aleph_2}}{\aleph_2}$.

(b) X_0 *behaves as a source under either of the following conditions:*

(b1) *When* $-2\sqrt{\aleph_2} \leqslant \aleph_1 < 0$ *and* $\delta > -\frac{\aleph_1}{\aleph_2}$.

(b2) *When* $\aleph_1 < -2\sqrt{\aleph_2}$ *and* $\delta > \frac{-\aleph_1+\sqrt{\aleph_1^2-4\aleph_2}}{\aleph_2}$ *or* $\aleph_1 \geqslant 0$.

(c) X_0 *behaves as a saddle if* $\aleph_1 < -2\sqrt{\aleph_2}$ *and* $\frac{-\aleph_1-\sqrt{\aleph_1^2-4\aleph_2}}{\Lambda_2} < \delta < \frac{-\aleph_1+\sqrt{\aleph_1^2-4\aleph_2}}{\aleph_2}$.

(d) X_0 *is non-hyperbolic under either of the following conditions:*

(d1) *When* $\aleph_1^2 \geq 4\aleph_2$, $\delta = \frac{-\aleph_1\pm\sqrt{\aleph_1^2-4\aleph_2}}{\aleph_2}$.

(d2) *When* $\aleph_1^2 < 4\aleph_2$ *and* $\delta = -\frac{\aleph_1}{\aleph_2}$.

According to Theorem 5, when condition (d1) holds, one of the eigenvalues of the positive fixed point X_0 is $\lambda_1 = -1$, while the other eigenvalue, λ_2, does not equal 1 in magnitude. Conversely, when condition (d2) of Theorem 3.1 holds, we can deduce that the eigenvalues of the positive fixed point X_0 constitute a pair of conjugate complex numbers with a modulus of 1.

Expanding upon this, in case (d1), one eigenvalue is real and equals -1, indicating a marginal stability along that direction, while the other eigenvalue is not restricted to the unit circle, implying a different behavior along the corresponding eigenvector. In case (d2), the eigenvalues are purely imaginary, suggesting a periodic or oscillatory behavior around the fixed point.

Now, we let

$$\begin{aligned}\Xi_1 = \{&(r, e, \gamma, \upsilon, t_h, k, c, p, q, m_1, m_2, m, \delta) :\\ &\delta = \frac{-\aleph_1 - \sqrt{\aleph_1^2 - 4\aleph_2}}{\aleph_2},\\ &\aleph_1 < -2\sqrt{\aleph_2}, \quad r, e, \gamma, \upsilon, t_h,\\ &k, c, p, q, m_1, m_2, m, \delta > 0\}\end{aligned}$$

or

$$\begin{aligned}\Xi_2 = \{&(r, e, \gamma, \upsilon, t_h, k, c, p, q, m_1, m_2, m, \delta) :\\ &\delta = \frac{-\aleph_1 + \sqrt{\aleph_1^2 - 4\aleph_2}}{\aleph_2},\\ &\aleph_1 < -2\sqrt{\aleph_2}, \quad r, e, \gamma, \upsilon,\\ &t_h, k, c, p, q, m_1, m_2, m, \delta > 0\}\end{aligned}$$

As parameters undergo small variations within a neighborhood of Ξ_1 or Ξ_2, system (20) may undergo flip bifurcation at the fixed point X_0. Let $\Xi_3 = \{(r, e, \gamma, \upsilon, t_h, k, c, p, q, m_1, m_2, m, \delta) : \delta = -\frac{\aleph_1}{\aleph_2}, -2\sqrt{\aleph_2} < \aleph_1 < 0, r, e, \gamma, \upsilon, t_h, k, c, p, q, m_1, m_2, m, \delta > 0\}$ When parameters experience small variations within a neighborhood of Ξ_3, the fixed point X_0 may undergo Neimark–Sacker bifurcation.

5 Flip bifurcation and Neimark–Sacker bifurcation

In the field of ecology, both Flip bifurcations and Neimark–Sacker (N–S) bifurcations in discrete predator–prey systems play an important role. They reveal the abrupt changes and dynamic shifts that may occur in the system under specific conditions. These bifurcations are crucial to our understanding of ecosystem stability, resilience and evolution. Flip bifurcations reveal abrupt state transitions that may occur during predator–prey interactions, which may lead to ecosystem collapse or transformation, which in turn affects ecosystem structure and function. On the other hand, N–S bifurcations indicate stable regions of the system in parameter space, which is crucial for us to predict and manage ecosystem responses. Overall, the study of these bifurcations helps us to gain a comprehensive understanding of the dynamic behavior of ecosystems and provide guidance for practice and ecological conservation.

Therefore, in this section, we introduce the parameter δ as a bifurcation parameter to study the Flip bifurcation and N–S bifurcation of the positive fixed point X_0 in the discrete-time differential-algebraic bioeconomic system (20). This analysis makes use of the new normal form of discrete differential-algebraic systems [29], the central manifold theorem, and bifurcation theory [30–32].

We first check the system (20) at X_0 for flip bifurcation when the parameters vary in a small neighborhood of Ξ_1. Similar conclusions can be drawn for the alternative case Ξ_2.

Under condition (d1), we determine that one eigenvalue of the positive definite immobile point X_0 is $\lambda_1 = -1$ and the other is $\lambda_2 = 3+\Lambda_1\delta_1$, where $|\lambda_2| \neq 1$. The parameters $(r, e, \gamma, \upsilon, t_h, k, c, p, q, m_1, m_2, m, \delta_1)$ can be chosen arbitrarily from the set Ξ_1, where $\delta_1 = \frac{-\aleph_1-\sqrt{\aleph_1^2-4\aleph_2}}{\aleph_2}$. We introduce δ_0 as the bifurcation parameter, which satisfies $|\delta_0| \ll 1$, denoting a smaller perturbation parameter. In order to analyze the stability of the flip bifurcation, we combine the ideas in the

literature [30–32] with the system (24) and formulate the system (28) as follows:

$$\begin{cases} x \to x + (\delta_1 + \delta_0)\, x[r\left(1 - \frac{x}{k}\right) \\ -\frac{\gamma y}{\sqrt{x}(1+t_h\gamma\sqrt{x})} - \frac{qE}{m_1E+m_2x}] \\ y \to y + (\delta_1 + \delta_0)\, y[-\upsilon + \frac{e\gamma\sqrt{x}}{1+t_h\gamma\sqrt{x}}] \\ 0 = \frac{qE}{m_1E+m_2x}(px - c) - m. \end{cases} \tag{28}$$

Using the identical outcomes as outlined in Sect. 3, we can simplify system (28) to system (24). To scrutinize the stability of the flip bifurcation, we draw upon references such as [30–32] and, in tandem with (24), articulate the structure of system (28) as follows:

$$\begin{pmatrix} y_1 \\ y_2 \\ \delta_0 \end{pmatrix} \to \begin{pmatrix} g_1^{(1)} y_1 + g_2^{(1)} y_2 + g_{11}^{(1)} y_1^2 + g_{12}^{(1)} y_1 y_2 + g_{10}^{(1)} y_1\delta_0 \\ +g_{20}^{(1)} y_2\delta_0 + g_{110}^{(1)} y_1^2\delta_0 + g_{120}^{(1)} y_1 y_2\delta_0 + \cdots \\ g_1^{(2)} y_1 + g_2^{(2)} y_2 + g_{11}^{(2)} y_1^2 + g_{12}^{(2)} y_1 y_2 + g_{22}^{(2)} y_2^2 \\ +g_{111}^{(2)} y_1^3 + g_{112}^{(2)} y_1^2 y_2 + g_{122}^{(2)} y_1 y_2^2 \\ +g_{10}^{(2)} y_1\delta_0 + g_{20}^{(2)} y_2\delta_0 \\ +g_{110}^{(2)} y_1^2\delta_0 + g_{120}^{(2)} y_1 y_2\delta_0 + g_{220}^{(2)} y_2^2\delta_0 + g_{1110}^{(2)} y_1^3\delta_0 \\ +g_{1120}^{(2)} y_1^2 y_2\delta_0 + g_{1220}^{(2)} y_1 y_2^2\delta_0 + \cdots \\ \delta_0 \end{pmatrix}, \tag{29}$$

The expressions for $g_1^{(1)}, g_2^{(1)}, \ldots, g_{1220}^{(2)}$ can be obtained from (20) and (24), as presented in the literature [33]. The detailed process is omitted here:

$$\begin{aligned} g_1^{(1)} &= 1 + \frac{\delta_1 q p x_0 E_0}{(px_0 - c)(m_1E_0 + m_2x_0)} \\ &\quad -\frac{\delta_1 r}{k}x_0 + \frac{\delta_1\gamma y_0(1 + 2t_h\gamma\sqrt{x_0})}{2\sqrt{x_0}\left(1 + t_h\gamma\sqrt{x_0}\right)^2}, \\ g_{10}^{(1)} &= \frac{q p x_0 E_0}{(px_0 - c)(m_1E_0 + m_2x_0)} \\ &\quad -\frac{r}{k}x_0 + \frac{\gamma y_0(1 + 2t_h\gamma\sqrt{x_0})}{2\sqrt{x_0}\left(1 + t_h\gamma\sqrt{x_0}\right)^2}, \\ g_2^{(1)} &= -\frac{\delta_1\gamma\sqrt{x_0}}{1 + t_h\gamma\sqrt{x_0}}, \\ g_{20}^{(1)} &= -\frac{\gamma\sqrt{x_0}}{1 + t_h\gamma\sqrt{x_0}}, \\ g_1^{(2)} &= \frac{\delta_1 e\gamma y_0}{2\sqrt{x_0}\left(1 + t_h\gamma\sqrt{x_0}\right)^2}, \\ g_{10}^{(2)} &= \frac{e\gamma y_0}{2\sqrt{x_0}\left(1 + t_h\gamma\sqrt{x_0}\right)^2}, \\ g_2^{(2)} &= 1, \quad g_{20}^{(2)} = 0, \\ g_{11}^{(1)} &= \frac{\delta_1\gamma y_0(1 + 3t_h\gamma\sqrt{x_0})}{4x_0^{\frac{3}{2}}(1 + t_h\gamma\sqrt{x_0})^3} \\ &\quad -\frac{2\delta_1 r}{k} + \frac{2\delta_1 E_0^2 m_1 m_2 q}{(m_1E_0 + m_2x_0)^3} \\ &\quad -\frac{2\delta_1 E_0 q\,(m_1 pE_0 + m_2c)\left(cm_1E_0 + m_2p^2x_0\right)}{(px_0 - c)^2\,(m_1E_0 + m_2x_0)^3}, \end{aligned} \tag{30}$$

$$\begin{aligned} g_{110}^{(1)} &= \frac{\gamma y_0(1 + 3t_h\gamma\sqrt{x_0})}{4x_0^{\frac{3}{2}}(1 + t_h\gamma\sqrt{x_0})^3} - \frac{2r}{k} + \frac{2E_0^2 m_1 m_2 q}{(m_1E_0 + m_2x_0)^3} \\ &\quad -\frac{2E_0 q\,(m_1 pE_0 + m_2c)\left(cm_1E_0 + m_2p^2x_0\right)}{(px_0 - c)^2\,(m_1E_0 + m_2x_0)^3}, \\ g_{12}^{(1)} &= -\frac{\gamma\delta_1}{2\sqrt{x_0}(1 + t_h\gamma\sqrt{x_0})}, \\ g_{120}^{(1)} &= -\frac{\gamma}{2\sqrt{x_0}(1 + t_h\gamma\sqrt{x_0})}, \\ g_{11}^{(2)} &= \frac{\delta_1\gamma e y_0(1 + 3t_h\gamma\sqrt{x_0})}{8x_0^{\frac{3}{2}}(1 + t_h\gamma\sqrt{x_0})^3}, \\ g_{110}^{(2)} &= \frac{\gamma e y_0(1 + 3t_h\gamma\sqrt{x_0})}{8x_0^{\frac{3}{2}}(1 + t_h\gamma\sqrt{x_0})^3}, \\ g_{12}^{(2)} &= \frac{e\gamma\delta_1}{2\sqrt{x_0}(1 + t_h\gamma\sqrt{x_0})}, \\ g_{120}^{(2)} &= \frac{e\gamma}{2\sqrt{x_0}(1 + t_h\gamma\sqrt{x_0})}, \\ g_{22}^{(2)} &= 0, \quad g_{220}^{(2)} = 0, \\ g_{111}^{(2)} &= -\frac{\gamma e\delta_1 y_0(4t_h\gamma\sqrt{x_0} + 5t_h^2\gamma^2x_0 + 1)}{8x_0^{\frac{5}{2}}(1 + t_h\gamma\sqrt{x_0})^4}, \\ g_{1110}^{(2)} &= -\frac{\gamma e y_0(4t_h\gamma\sqrt{x_0} + 5t_h^2\gamma^2x_0 + 1)}{8x_0^{\frac{5}{2}}(1 + t_h\gamma\sqrt{x_0})^4}, \\ g_{112}^{(2)} &= -\frac{\gamma e\delta_1 y_0(1 + 3t_h\gamma\sqrt{x_0})}{8x_0^{\frac{3}{2}}(1 + t_h\gamma\sqrt{x_0})^3}, \\ g_{1120}^{(2)} &= -\frac{\gamma e y_0(1 + 3t_h\gamma\sqrt{x_0})}{8x_0^{\frac{3}{2}}(1 + t_h\gamma\sqrt{x_0})^3}, \\ g_{122}^{(2)} &= 0, \quad g_{1220}^{(2)} = 0, \\ g_{22}^{(1)} &= g_{220}^{(1)} = \cdots = g_{222}^{(2)} = g_{2220}^{(2)} = 0. \end{aligned}$$

Now, through the application of the following translation

$$\begin{pmatrix} y_1 \\ y_2 \\ \delta_0 \end{pmatrix} = \begin{pmatrix} g_2^{(1)} & g_2^{(1)} & 0 \\ -1 - g_1^{(1)} & \lambda_2 - g_1^{(1)} & 0 \\ 0 & 0 & 1 \end{pmatrix} \begin{pmatrix} z_1 \\ z_2 \\ \mu_0 \end{pmatrix}, \tag{31}$$

Subsequently, the normal form of (29) can be derived as follows:

$$\begin{pmatrix} z_1 \\ z_2 \\ \mu_0 \end{pmatrix}$$

$$\rightarrow \begin{pmatrix} -z_1+\bar{g}_{11}^{(1)}z_1^2+\bar{g}_{12}^{(1)}z_1z_2+\bar{g}_{10}^{(1)}z_1\mu_0+\bar{g}_{20}^{(1)}z_2\mu_0 \\ +\bar{g}_{10}^{(1)}z_1^2\mu_0+\bar{g}_{120}^{(1)}z_1z_2\mu_0+\cdots \\ \lambda_2 z_2+\bar{g}_{11}^{(2)}z_1^2+\bar{g}_{12}^{(2)}z_1z_2+\bar{g}_{22}^{(2)}z_2^2+\bar{g}_{111}^{(2)}z_1^3 \\ +\bar{g}_{112}^{(2)}z_1^2z_2+\bar{g}_{122}^{(2)}z_1z_2^2+\bar{g}_{10}^{(2)}z_1\mu_0+\bar{g}_{20}^{(2)}z_2\mu_0 \\ +\bar{g}_{110}^{(2)}z_1^2\mu_0+\bar{g}_{120}^{(2)}z_1z_2\mu_0+\bar{g}_{220}^{(2)}z_2^2\mu_0+\bar{g}_{1110}^{(2)}z_1^3\mu_0 \\ +\bar{g}_{1120}^{(2)}z_1^2z_2\mu_0+\bar{g}_{1220}^{(2)}z_1z_2^2\mu_0+\cdots \\ \mu_0 \end{pmatrix} \tag{32}$$

where

$$\begin{aligned}
\bar{g}_{11}^{(1)} =& \frac{1}{1+\lambda_2}\left\{\left(\lambda_2-g_1^{(1)}\right)\left[g_{11}^{(1)}g_2^{(1)}-g_{12}^{(1)}\left(1+g_1^{(1)}\right)\right]\right. \\
&-g_{11}^{(2)}\left(g_2^{(1)}\right)^2 \\
&\left.+g_{12}^{(2)}g_2^{(1)}\left(1+g_1^{(1)}\right)-g_{22}^{(2)}\left(1+g_1^{(1)}\right)^2\right\}, \\
\bar{g}_{10}^{(1)} =& \frac{1}{1+\lambda_2}\left\{\left(\lambda_2-g_1^{(1)}\right)\left[g_{10}^{(1)}-g_{20}^{(1)}\left(1+g_1^{(1)}\right)/g_2^{(1)}\right]\right. \\
&\left.-g_{10}^{(2)}g_2^{(1)}+g_{20}^{(2)}\left(1+g_1^{(1)}\right)\right\}, \\
\bar{g}_{12}^{(1)} =& \frac{1}{1+\lambda_2}\left\{\left(\lambda_2-g_1^{(1)}\right)\left[2g_{11}^{(1)}g_2^{(1)}\right.\right. \\
&\left.+g_{12}^{(1)}\left(\lambda_2-1-2g_1^{(1)}\right)\right]-2g_{11}^{(2)}\left(g_2^{(1)}\right)^2 \\
&-g_{12}^{(2)}g_2^{(1)}\left(\lambda_2-1-2g_1^{(1)}\right) \\
&\left.+2g_{22}^{(2)}\left(1+g_1^{(1)}\right)\left(\lambda_2-g_1^{(1)}\right)\right\}, \\
\bar{g}_{20}^{(1)} =& \frac{1}{1+\lambda_2}\left\{\left(\lambda_2-g_1^{(1)}\right)\left[g_{10}^{(1)}+g_{20}^{(1)}\left(\lambda_2-g_1^{(1)}\right)/g_2^{(1)}\right]\right. \\
&\left.-g_{10}^{(2)}g_2^{(1)}-g_{20}^{(2)}\left(\lambda_2-g_1^{(1)}\right)\right\}, \\
\bar{g}_{110}^{(1)} =& \frac{1}{1+\lambda_2}\left\{\left(\lambda_2-g_1^{(1)}\right)\left[g_{110}^{(1)}g_2^{(1)}-g_{120}^{(1)}\left(1+g_1^{(1)}\right)\right]\right. \\
&-g_{110}^{(2)}\left(g_2^{(1)}\right)^2 \\
&\left.+g_{120}^{(2)}g_2^{(1)}\left(1+g_1^{(1)}\right)-g_{220}^{(2)}\left(1+g_1^{(1)}\right)^2\right\}, \\
\bar{g}_{10}^{(2)} =& \frac{1}{1+\lambda_2}\left\{\left(1+g_1^{(1)}\right)\left[g_{10}^{(1)}-g_{20}^{(1)}\left(1+g_1^{(1)}\right)/g_2^{(1)}\right]\right. \\
&\left.+g_{10}^{(2)}g_2^{(1)}-g_{20}^{(2)}\left(1+g_1^{(1)}\right)\right\}, \\
\bar{g}_{11}^{(2)} =& \frac{1}{1+\lambda_2}\left\{\left(1+g_1^{(1)}\right)\left[g_{11}^{(1)}g_2^{(1)}-g_{12}^{(1)}\left(1+g_1^{(1)}\right)\right]\right. \\
&+g_{11}^{(2)}\left(g_2^{(1)}\right)^2 \\
&\left.-g_{12}^{(2)}g_2^{(1)}\left(1+g_1^{(1)}\right)+g_{22}^{(2)}\left(1+g_1^{(1)}\right)^2\right\}, \\
&\cdots \\
\bar{g}_{22}^{(2)} =& \quad \ldots=\bar{g}_{222}^{(2)}=0.
\end{aligned}$$

Let's utilize the center manifold to analyze the dynamics of (32) around the fixed point (0,0) within a small vicinity of $\mu_0=0$. According to the center manifold theorem [31], we establish that (32) exhibits a center manifold described by:

$$\begin{aligned}
W^c(0,0,0) =& \left\{(z_1,z_2,\mu_0)\in R^3 : z_2=c_1z_1^2\right. \\
&\left.+c_2z_1\mu_0+c_3\mu_0^2+o\left((|z_1|+|\mu_0|)^3\right)\right\}.
\end{aligned}$$

Upon substituting the center manifold into (32), we deduce:

$$c_1=\frac{\bar{g}_{11}^{(2)}}{1-\lambda_2},\quad c_2=-\frac{\bar{g}_{10}^{(2)}}{1+\lambda_2},\quad c_3=0$$

Hence, the map (32) restricted to the center manifold $W^c(0,0,0)$ is expressed as:

$$\begin{aligned}
\Phi : z_1 \rightarrow & -z_1+\varpi_1z_1^2+\varpi_2z_1\mu_0+\varpi_3z_1^2\mu_0 \\
&+\varpi_4z_1\mu_0^2+\varpi_5z_1^3+o\left((|z_1|+|\mu_0|)^4\right).
\end{aligned} \tag{33}$$

where

$$\begin{aligned}
\varpi_1 =& \bar{g}_{11}^{(1)},\quad \varpi_2=\bar{g}_{10}^{(1)}, \\
\varpi_3 =& \frac{\bar{g}_{20}^{(1)}\bar{f}_{11}^{(2)}(1+\lambda_2)-\bar{g}_{10}^{(2)}\bar{f}_{12}^{(1)}(1-\lambda_2)}{1-\lambda_2^2}+\bar{g}_{110}^{(1)}, \\
\varpi_4 =& -\frac{\bar{g}_{20}^{(1)}\bar{g}_{10}^{(2)}}{1+\lambda_2},\quad \varpi_5=\frac{\bar{g}_{12}^{(1)}\bar{g}_{11}^{(2)}}{1-\lambda_2}.
\end{aligned}$$

For the map (32) to undergo a flip bifurcation, it is necessary for two discriminant quantities ς_1 and ς_2 to be non-zero, where:

$$\begin{aligned}
\varsigma_1 =& \left(\frac{\partial^2\Phi}{\partial z_1\partial\mu_0}+\frac{1}{2}\frac{\partial\Phi}{\partial\mu_0}\frac{\partial^2\Phi}{\partial z_1^2}\right)\Bigg|_{(0,0)}=\varpi_2, \\
\varsigma_2 =& \left(\frac{1}{6}\frac{\partial^3\Phi}{\partial z_1^3}+\left(\frac{1}{2}\frac{\partial^2\Phi}{\partial z_1^2}\right)^2\right)\Bigg|_{(0,0)}=\varpi_5+\varpi_1^2.
\end{aligned}$$

Based on the analysis provided above and the theorem established in references [30–32], we can infer the following outcome.

Theorem 6 *According to Lemma 1 and condition (d1) of Theorem 5, if $\varsigma_1\varsigma_2\neq 0$, then the system (20) will undergo a flipping bifurcation at the immovable point X_0 when the parameter δ varies in a small neighborhood of δ_1. Furthermore, if $\varsigma_2>0$, then the period-2 orbit from X_0 is a stable state. Conversely, if $\varsigma_2<0$, then the period-2 orbit from X_0 is unstable states.*

This theorem clarifies the occurrence of a flip bifurcation at the fixed point X_0 of system (20) under specific conditions, providing insights into the stability of the resulting period-2 orbits based on the sign of ς_2. In the following segment of this section, we investigate the stability of the Neimark–Sacker bifurcation as parameters undergo variations within a narrow vicinity of Ξ_3.

Considering $(r,k,t_h,\gamma,\upsilon,e,p,q,c,m_1,m_2,m,\delta_2)\in\Xi_3$ where $\delta_2=-\frac{\aleph_1}{\aleph_2}$, let $\bar{\delta}_0$ ($|\bar{\delta}_0|\ll 1$) be selected as the bifurcation parameter. We analyze the perturbation of (20) as follows:

$$\begin{cases}
x\rightarrow x+\left(\delta_2+\bar{\delta}_0\right)x[r\left(1-\frac{x}{k}\right) \\
-\frac{\gamma y}{\sqrt{x}(1+t_h\gamma\sqrt{x})}-\frac{qE}{m_1E+m_2x}] \\
y\rightarrow y+\left(\delta_2+\bar{\delta}_0\right)y[-\upsilon+\frac{e\gamma\sqrt{x}}{1+t_h\gamma\sqrt{x}}] \\
0=\frac{qE}{m_1E+m_2x}(px-c)-m.
\end{cases} \tag{34}$$

To evaluate the stability of the N–S bifurcation, we refer to the established literature [30–32] and, utilizing equations (24) and (34), describe the configuration of system (34) as follows:

$$\begin{pmatrix} y_1 \\ y_2 \end{pmatrix} \to \begin{pmatrix} g_1^{(1)} y_1 + g_2^{(1)} y_2 + g_{11}^{(1)} y_1^2 + g_{12}^{(1)} y_1 y_2 + \cdots \\ g_1^{(2)} y_1 + g_2^{(2)} y_2 + g_{11}^{(2)} y_1^2 + g_{12}^{(2)} y_1 y_2 + g_{22}^{(2)} y_2^2 \\ + g_{111}^{(2)} y_1^3 + g_{112}^{(2)} y_1^2 y_2 + g_{122}^{(2)} y_1 y_2^2 + \cdots \end{pmatrix}. \tag{35}$$

The coefficients $g_1^{(1)}, g_2^{(1)}, \ldots, g_{122}^{(2)}$ provided in (30) only require $\delta_1 = \delta_2$. It's important to emphasize that the characteristic equation derived from the linearization of the map (34) at $Y_0 = (0, 0)$ is formulated as follows:

$$\begin{aligned} &\lambda^2 - \left[2 + \aleph_1 \left(\delta_2 + \bar{\delta}_0\right)\right]\lambda \\ &+ \left[1 + \aleph_1 \left(\delta_2 + \bar{\delta}_0\right) + \aleph_2 \left(\delta_2 + \bar{\delta}_0\right)^2\right] = 0, \end{aligned} \tag{36}$$

As per the findings in [39] and condition (d2) of Theorem 3.1, it is established that the eigenvalues for (20) at Y_0 consist of a pair of complex conjugate numbers λ and $\bar{\lambda}$, each with a modulus of 1. Additionally,

$$\begin{aligned} &|\lambda| = \sqrt{\left[1 + \aleph_1 \left(\delta_2 + \bar{\delta}_0\right) + \aleph_2 \left(\delta_2 + \bar{\delta}_0\right)^2\right]}, \\ &l = \left.\frac{d|\lambda|}{d\bar{\delta}_0}\right|_{\bar{\delta}_0=0} = -\frac{\aleph_1}{2} > 0. \end{aligned} \tag{37}$$

Furthermore, in the case where $\bar{\delta}_0 = 0$, we need to ensure that λ^i and $\bar{\lambda}^i \neq 1$ (for $i = 1, 2, 3, 4$), which is equivalent to $-(2 + \aleph_1\delta_2) \neq -2, 0, 1, 2$. Specifically, it suffices to ensure that $-(2 + \aleph_1\delta_2) \neq 0, 1$, resulting in $\frac{\aleph_1^2}{\aleph_2} \neq 2, 3$. Consequently, the eigenvalues λ and $\bar{\lambda}$ of the fixed point Y_0 from (35) do not intersect the unit circle with the coordinate axes when $\bar{\delta}_0 = 0$.

Next, we delve into the analysis of the normal form of the map (36) at $\bar{\delta}_0 = 0$. Setting $\bar{\delta}_0 = 0, \mu = 1 + \frac{\aleph_1\delta_2}{2}, \kappa = \frac{\delta_2}{2}\sqrt{4\aleph_2 - \aleph_1^2}$, and then, employing the translation:

$$\begin{pmatrix} y_1 \\ y_2 \end{pmatrix} = \begin{pmatrix} g_2^{(1)} & 0 \\ \mu - g_1^{(1)} & -\kappa \end{pmatrix} \begin{pmatrix} z_1 \\ z_2 \end{pmatrix}, \tag{38}$$

then, we can get the normal form of (35) as follows:

$$\begin{pmatrix} z_1 \\ z_2 \end{pmatrix} \to \begin{pmatrix} \mu z_1 - \kappa z_2 + \widehat{g}_{11}^{(1)} z_1^2 + \widehat{g}_{12}^{(1)} z_1 z_2 + \cdots \\ \kappa z_1 + \mu z_2 + \widehat{g}_{11}^{(2)} z_1^2 + \widehat{g}_{12}^{(2)} z_1 z_2 + \widehat{g}_{22}^{(2)} z_2^2 \\ + \widehat{g}_{111}^{(2)} z_1^3 + \widehat{g}_{112}^{(2)} z_1^2 z_2 + \widehat{g}_{122}^{(2)} z_1 z_2^2 + \cdots \end{pmatrix}, \tag{39}$$

where

$$\begin{aligned} \widehat{g}_{11}^{(1)} =& g_2^{(1)} g_{11}^{(1)} + g_{12}^{(1)} \left(\mu - g_1^{(1)}\right), \\ \widehat{g}_{12}^{(1)} =& -\kappa g_{12}^{(1)}, \\ \widehat{g}_{11}^{(2)} =& \frac{1}{\kappa}\left[g_{11}^{(1)} g_2^{(1)} \left(\mu - g_1^{(1)}\right) \right. \\ &+ \left(g_{12}^{(1)} - g_2^{(2)}\right)\left(\mu - g_1^{(1)}\right)^2 \\ &\left. - g_{11}^{(2)} \left(g_2^{(1)}\right)^2 - g_{12}^{(2)} g_2^{(1)} \left(\mu - g_1^{(1)}\right)\right], \\ \widehat{g}_{12}^{(2)} =& \left(2g_2^{(2)} - g_{12}^{(1)}\right)\left(\mu - g_1^{(1)}\right) + g_{12}^{(2)} g_2^{(1)}, \\ \widehat{g}_{22}^{(2)} =& -\kappa g_2^{(2)}, \\ \widehat{g}_{111}^{(2)} =& -\frac{1}{\kappa}\left[g_{111}^{(2)} \left(g_2^{(1)}\right)^3 + g_{112}^{(2)} \left(g_2^{(1)}\right)^2 \left(\mu - g_1^{(1)}\right) \right. \\ &\left. + g_{122}^{(2)} \left(g_2^{(1)}\right)^2 \left(\mu - g_1^{(1)}\right)^2\right], \\ \widehat{g}_{112}^{(2)} =& g_{112}^{(2)} \left(g_2^{(1)}\right)^2 + 2g_{122}^{(2)} g_2^{(1)} \left(\mu - g_1^{(1)}\right), \\ \widehat{g}_{122}^{(2)} =& -\kappa g_{122}^{(2)} g_2^{(1)}, \\ \widehat{g}_{22}^{(1)} =& \cdots = \widehat{g}_{222}^{(2)} = 0, \quad \delta_1 = \delta_2. \end{aligned}$$

To trigger the N–S bifurcation in map (20), as the works of [30–32], it's essential that the discriminant quantity doesn't equal zero. This condition is crucial for inducing the bifurcation phenomenon.

$$\begin{aligned} \varsigma_0 =& \left\{-\mathrm{Re}\left[\frac{(1-2\lambda)\bar{\lambda}^2}{1-\lambda}\zeta_{11}\zeta_{20}\right] \right. \\ &\left. - \frac{1}{2}|\zeta_{11}|^2 - |\zeta_{02}|^2 + \mathrm{Re}(\bar{\lambda}\zeta_{21})\right\}\Big|_{\delta_0=0}, \end{aligned} \tag{40}$$

where

$$\begin{aligned} \zeta_{11} =& \frac{1}{4}\left[\widehat{g}_{11}^{(1)} + \widehat{g}_{22}^{(1)} + i\left(\widehat{g}_{11}^{(2)} + \widehat{g}_{22}^{(2)}\right)\right], \\ \zeta_{20} =& \frac{1}{8}\left[\widehat{g}_{11}^{(1)} - \widehat{g}_{22}^{(1)} + 2\widehat{g}_{12}^{(2)} + \mathrm{i}\left(\widehat{g}_{11}^{(2)} - \widehat{g}_{22}^{(2)} - 2\widehat{g}_{12}^{(1)}\right)\right], \\ \zeta_{02} =& \frac{1}{8}\left[\widehat{g}_{11}^{(1)} - \widehat{g}_{22}^{(1)} - 2\widehat{g}_{12}^{(2)} + i\left(\widehat{g}_{11}^{(2)} - \widehat{g}_{22}^{(2)} + 2\widehat{g}_{12}^{(1)}\right)\right], \\ \zeta_{21} =& \frac{1}{16}\left[\widehat{g}_{111}^{(1)} + \widehat{g}_{122}^{(1)} + \widehat{g}_{112}^{(2)} + \widehat{g}_{222}^{(2)} \right. \\ &\left. + i\left(\widehat{g}_{111}^{(2)} + \widehat{g}_{122}^{(2)} - \widehat{g}_{112}^{(1)} - \widehat{g}_{222}^{(1)}\right)\right]. \end{aligned}$$

Summarizing above results and the theorem in [30–32], here's a rephrased and expanded version of the above results and theorem:

Theorem 7 *Under the conditions specified in Theorem 5, denoted as (d2), and with parameters* $(r, k, t_h, \gamma, \upsilon, e, p, q, c, m_1, m_2, m, \delta_2)$ *belonging to the set* Ξ_3, *if* $l = \left.\frac{d|\lambda|}{d\bar{\delta}_0}\right|_{\bar{\delta}_0=0} = -\frac{\aleph_1}{2} > 0$, *and* $\frac{\aleph_1^2}{\aleph_2} \neq 2, 3$, *while* $\varsigma_0 \neq 0$, *then system (20) undergoes a Neimark–Sacker bifurcation at the positive fixed point* X_0 *as the parameter* δ *varies within a small vicinity of* δ_2. *Additionally, if* $\varsigma_0 < 0$, *an attracting invariant closed curve*

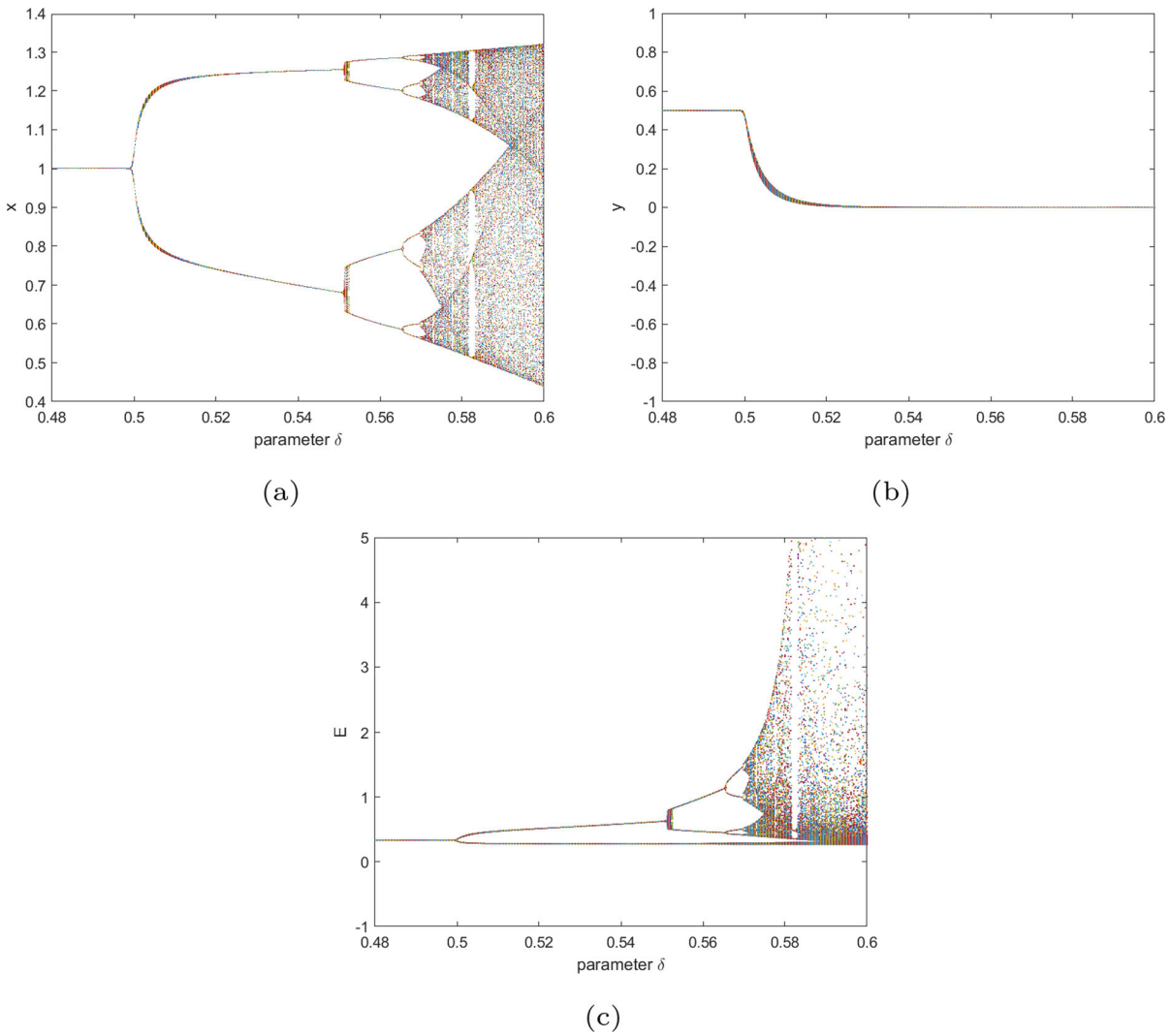

Fig. 1 **a** Bifurcation diagram in the (δ, x) plane visualizes how the parameter δ influences the variable x. **b** Bifurcation diagram in the (δ, y) plane illustrates the relationship between the parameter δ and the variable y. **c** Bifurcation diagram in the (δ, E) plane shows the dependency between the parameter δ and the system's energy E

emerges from the fixed point for $\delta > \delta_2$, whereas if $\varsigma_0 > 0$, a repelling invariant closed curve arises from the fixed point for $\delta < \delta_2$.

6 Codimension-two bifurcation analysis

To further investigate the dynamic behavior of the system (20), we investigated its codimension-two bifurcations. Let $\lambda_{1,2}$ be two eigenvalues of Jacobian matrix $D_Y f(\Psi(0))$. It follows that $\lambda_1\lambda_2 = 1$, and that implies that $\lambda_{1,2} = e^{\pm i\theta_0}$ for some real number θ_0. If $\lambda_{1,2}^k = 1$ for $k = 1, 2, 3, 4$, system (20) may exhibit more complicated dynamical behaviors, namely, chaos and codimension-2 bifurcations. As a matter of fact. we can get the following conditions for the strong resonances. Thus, we define one bifurcation set

$$F_{12} = \Big\{(r, e, \gamma, \upsilon, t_h, k, c, p, q, m_1, m_2, m, \delta) : \delta = \frac{-4}{\aleph_1},$$
$$e = \frac{8(1 + t_h\gamma\sqrt{x_0})^3}{\gamma^2 y_0},$$
$$r, e, \gamma, \upsilon, t_h, k, c, p, q, m_1, m_2, m, \delta > 0\}$$

In this section, we will give attention to recapitulate the codimension-two bifurcation of system (20) around X_0. Parameters δ, e are chosen as the bifurcation parameters.

By [36], the system (20) can be expressed as

$$\begin{bmatrix} y_1 \\ y_2 \end{bmatrix} \to \begin{bmatrix} -1+a_{10}(\bar{\delta},\bar{e}) & 1+a_{01}(\bar{\delta},\bar{e}) \\ b_{10}(\bar{\delta},\bar{e}) & -1+b_{01}(\bar{\delta},\bar{e}) \end{bmatrix} \begin{bmatrix} y_1 \\ y_2 \end{bmatrix} + \begin{bmatrix} f(y_1,y_2) \\ g(y_1,y_2) \end{bmatrix} \tag{41}$$

$$\begin{aligned}
a_{10} &= 2+\frac{\delta_1 q p x_0 E_0}{(p x_0-c)(m_1 E_0+m_2 x_0)}-\frac{\delta_1 r}{k}x_0 \\
&\quad +\frac{\delta_1\gamma y_0(1+2t_h\gamma\sqrt{x_0})}{2\sqrt{x_0}\left(1+t_h\gamma\sqrt{x_0}\right)^2}, \\
a_{01} &= -1-\frac{\delta_1\gamma\sqrt{x_0}}{1+t_h\gamma\sqrt{x_0}}, \\
b_{10} &= \frac{\delta_1 e\gamma y_0}{2\sqrt{x_0}\left(1+t_h\gamma\sqrt{x_0}\right)^2}, \\
b_{01} &= 2, \\
f(y_1,y_2) &= \Big(\frac{\delta_1\gamma y_0(1+3t_h\gamma\sqrt{x_0})}{4x_0^{\frac{3}{2}}(1+t_h\gamma\sqrt{x_0})^3}-\frac{2\delta_1 r}{k} \\
&\quad +\frac{2\delta_1 E_0^2 m_1 m_2 q}{(m_1E_0+m_2x_0)^3} \\
&\quad -\frac{2\delta_1 E_0 q\,(m_1 p E_0+m_2 c)\left(c m_1 E_0+m_2 p^2 x_0\right)}{(p x_0-c)^2(m_1E_0+m_2x_0)^3}\Big)y_1^2 \\
&\quad -\left(-\frac{\gamma\delta_1}{2\sqrt{x_0}(1+t_h\gamma\sqrt{x_0})}\right)y_1y_2 \\
&= a_{20}y_1^2+a_{11}y_1y_2, \\
g(y_1,y_2) &= \left(\frac{\delta_1\gamma e y_0(1+3t_h\gamma\sqrt{x_0})}{8x_0^{\frac{3}{2}}(1+t_h\gamma\sqrt{x_0})^3}\right)y_1^2 \\
&\quad +\left(\frac{e\gamma\delta_1}{2\sqrt{x_0}(1+t_h\gamma\sqrt{x_0})}\right)y_1y_2 \\
&= b_{20}y_1^2+b_{11}y_1y_2
\end{aligned}$$

Introduce the non-singular linear coordinate transformation

$$\begin{bmatrix} y_1 \\ y_2 \end{bmatrix} \to \begin{bmatrix} 1+a_{01}(\bar{\delta},\bar{e}) & 0 \\ -a_{10}(\bar{\delta},\bar{e}) & 1 \end{bmatrix} \begin{bmatrix} y_1 \\ y_2 \end{bmatrix}.$$

Map (41) can be uniquely represented as

$$\begin{bmatrix} y_1 \\ y_2 \end{bmatrix} \to \begin{bmatrix} -1 & 1 \\ \theta_1(\bar{\delta},\bar{e}) & -1+\theta_2(\bar{\delta},\bar{e}) \end{bmatrix} \begin{bmatrix} y_1 \\ y_2 \end{bmatrix} + \begin{bmatrix} T(y_1,y_2) \\ P(y_1,y_2) \end{bmatrix},$$

where

$$\begin{aligned}
\theta_1 &= b_{10}+a_{01}b_{10}-a_{10}b_{01}, \\
\theta_2 &= a_{10}+b_{01}, \\
T(y_1,y_2) &= \left[a_{20}(1+a_{01})-a_{10}a_{11}\right]y_1^2 \\
&\quad +a_{11}y_1y_2 = t_{20}y_1^2+t_{11}y_1y_2, \\
P(y_1,y_2) &= \left[a_{20}(1+a_{01})a_{10}-a_{10}^2a_{11}\right. \\
&\quad \left.+b_{20}(1+a_{01})^2-a_{10}b_{11}(1+a_{01})\right]y_1^2 \\
&\quad +\left[a_{11}a_{10}+b_{11}(1+a_{01})\right]y_1y_2 \\
&= p_{20}y_1^2+p_{11}y_1y_2.
\end{aligned}$$

Then we take

$$y_1 = w_1+\sum_{2\le j+k\le 3}\varphi_{jk}(\bar{\lambda},\bar{e})w_1^j w_2^k,$$

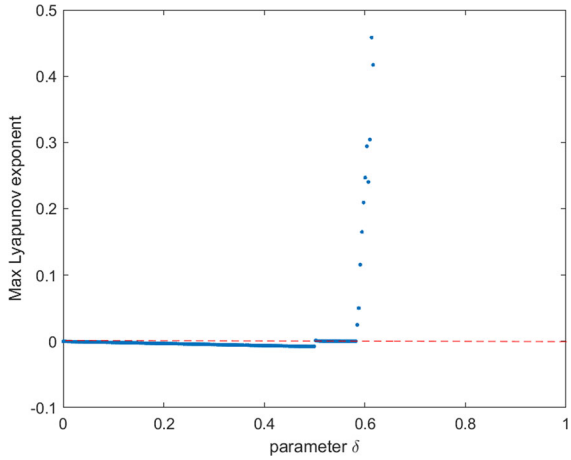

Fig. 2 The maximum Lyapunov exponents corresponding to Fig. 1a–c

$$y_2 = w_2+\sum_{2\le j+k\le 3}\omega_{jk}(\bar{\lambda},\bar{e})w_1^j w_2^k,$$

with

$$\begin{aligned}
\varphi_{20} &= \frac{1}{2}t_{20}+\frac{1}{4}p_{20}, \\
\varphi_{11} &= \frac{1}{2}t_{20}+\frac{1}{2}t_{11}+\frac{1}{2}p_{20}+\frac{1}{4}p_{11}, \\
\varphi_{02} &= \frac{1}{4}g_{11}+\frac{1}{8}p_{20}+\frac{1}{4}p_{11}, \\
\omega_{20} &= \frac{1}{2}p_{20}, \\
\omega_{11} &= \frac{1}{2}p_{20}+\frac{1}{2}p_{11}, \\
\omega_{02} &= \frac{1}{4}p_{11}.
\end{aligned}$$

The normal form for 1:2 resonance can be achieved as follows

$$\begin{bmatrix} w_1 \\ w_2 \end{bmatrix} \to \begin{bmatrix} -1 & 1 \\ \theta_1(\bar{\delta},\bar{e}) & -1+\theta_2(\bar{\delta},\bar{e}) \end{bmatrix} \begin{bmatrix} w_1 \\ w_2 \end{bmatrix} + \begin{bmatrix} 0 \\ C(\bar{\delta},\bar{e})w_1^3+D(\bar{\delta},\bar{e})w_1^2w_2 \end{bmatrix},$$

where

$$\begin{aligned}
C(\bar{\delta},\bar{e}) &= t_{20}p_{20}+\frac{1}{2}p_{20}^2+\frac{1}{2}p_{20}p_{11}, \\
D(\bar{\delta},\bar{e}) &= \frac{1}{2}t_{20}p_{11}+\frac{5}{4}p_{20}p_{11}+\frac{5}{2}t_{20}p_{20} \\
&\quad +\frac{5}{2}p_{20}t_{11}+p_{20}^2+\frac{1}{2}p_{11}^2+3t_{20}^2.
\end{aligned}$$

Based on the results given in [40–42], We have the following theorem which gives parametric conditions at 1: 2 resonance point.

Theorem 8 *Assume that* $C(\bar{\delta},\bar{e})\neq 0$ *and* $D(\bar{\delta},\bar{e})+3C(\bar{\delta},\bar{e})\neq 0$. *Then model* (20) *undergoes a 1: 2 strong resonance bifurcation at* X_0 *when parameters vary in a small neighbourhood*

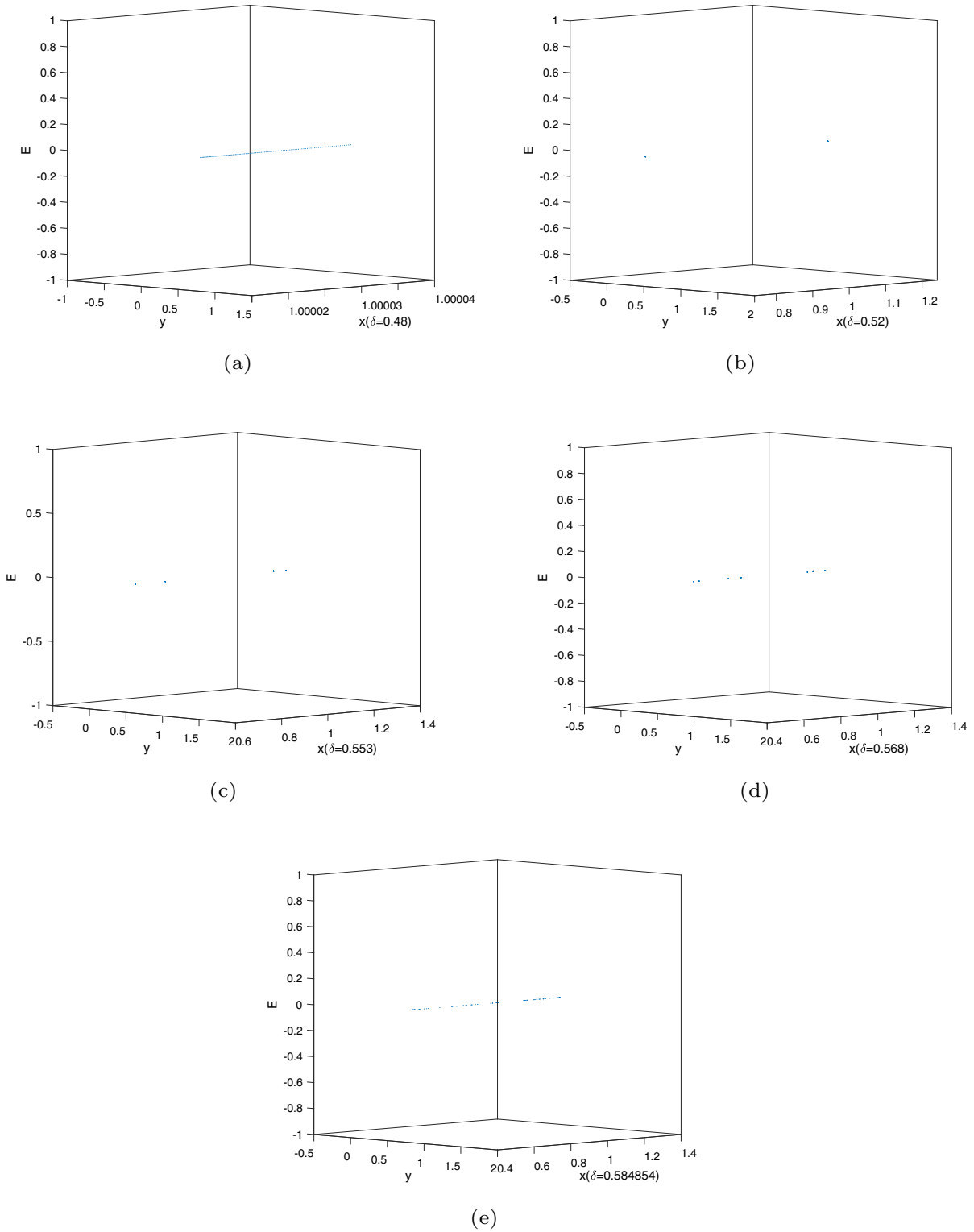

Fig. 3 Phase portraits for various values of δ corresponding to Fig. 1 are as follows: **a** $\delta = 0.48$, **b** $\delta = 0.52$, **c** $\delta = 0.553$, **d** $\delta = 0.568$, **e** $\delta = 0.584854$

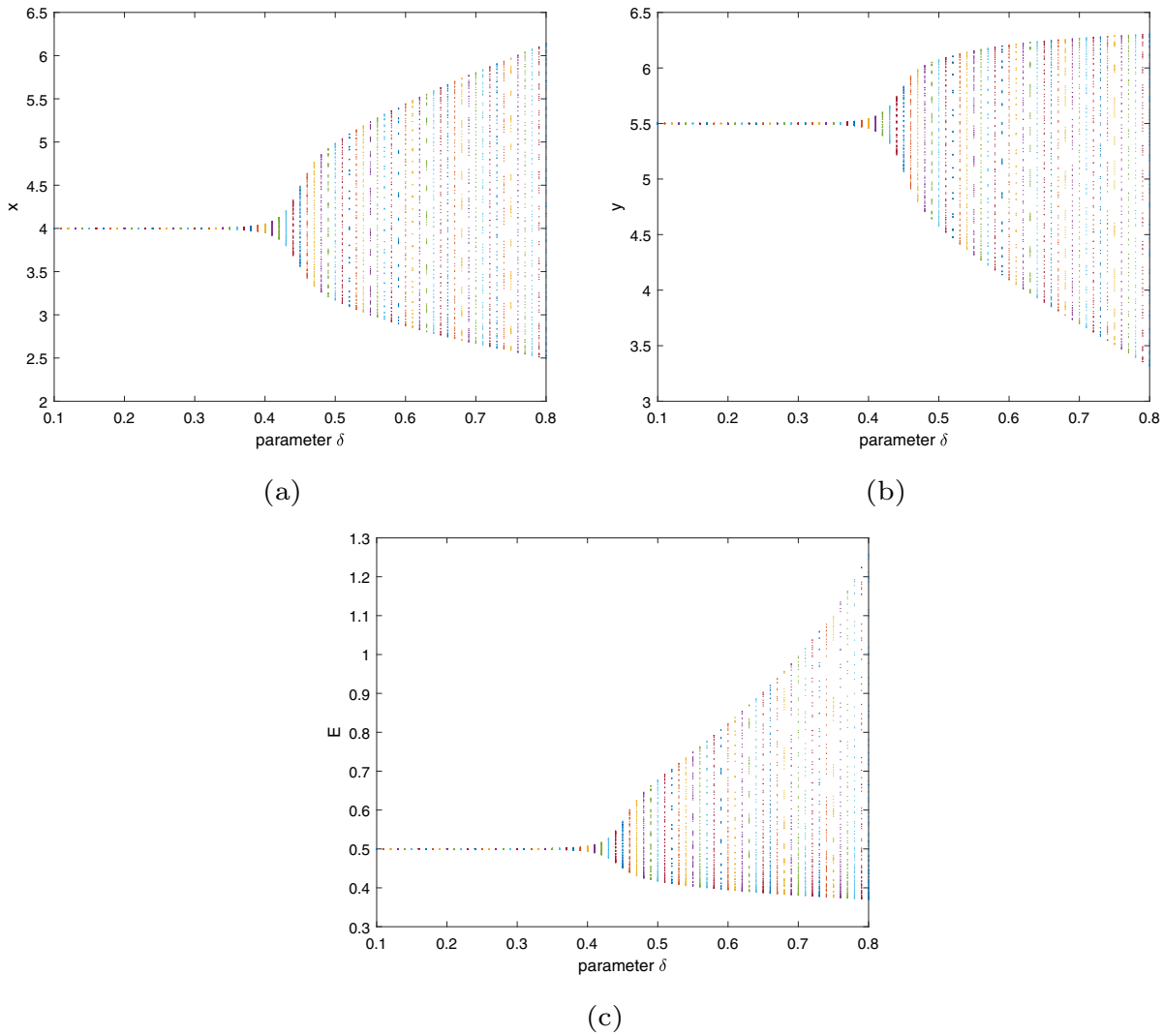

Fig. 4 **a** Bifurcation diagram in the (δ, x) plane visualizes how the parameter δ influences the variable x. **b** Bifurcation diagram in the (δ, y) plane illustrates the relationship between the parameter δ and the variable y. **c** Bifurcation diagram in the (δ, E) plane shows the dependency between the parameter δ and the system's energy E

of F_{12}. *If we further assume* $C(\bar{\delta}, \bar{e}) < 0$ *(resp.,* $C(\bar{\delta}, \bar{e}) > 0$ *), then* X_0 *is a saddle (resp., elliptic).* $D(\bar{\delta}, \bar{e}) + 3C(\bar{\delta}, \bar{e})$ *determines the bifurcation scenarios near the 1: 2 point. Moreover, model (1.4) has the following bifurcation behaviors:*

(I) *There is a pitchfork bifurcation curve* $LY = \left\{(\theta_1, \theta_2) : \theta_1 = 0\right\}$, *and there exists nontrivial fixed point for* $\theta_1 < 0$;

(II) *There is a non-degenerate Neimark–Sacker bifurcation curve* $P = \{(\theta_1, \theta_2) : \theta_1 = -\theta_2 + O\left((|\theta_1| + |\theta_2|)^2\right), \theta_1 < 0\}$;

(III) *There is a heteroclinic bifurcation curve* $PV = \left\{(\theta_1, \theta_2) : \theta_1 = -\frac{5}{3}\theta_2 + O\left((|\theta_1| + |\theta_2|)^2\right), \theta_1 < 0\right\}$.

7 Numerical simulation

Example 5.1 (**Flip bifurcation**) For the parameters $r = \frac{19}{4}, k = \frac{38}{35}, t_h = 1, \upsilon = 1, \gamma = 1, q = 1, e = 2, c = 1, m_1 = 2, m_2 = 2, m = \frac{1}{4}, p = 3$ and δ varying between 0.48 to 0.6 range, the fixed point $X_0 = (1, \frac{1}{2}, \frac{1}{3})$ appears to flip bifurcation at $\delta_1 = 0.5039$ with eigenvalues of $\varsigma_1 = 3837 * 10^3$ and $\varsigma_2 = -3.0329 * 10^6$. This result confirms the effectiveness of Theorem 3.

By analyzing Fig. 1a–c, we can clearly observe that the fixed point $X_0 = (1, \frac{1}{2}, \frac{1}{3})$ demonstrates an unstable state at $\delta < 0.504$ and remains instability at the flip bifurcation param-

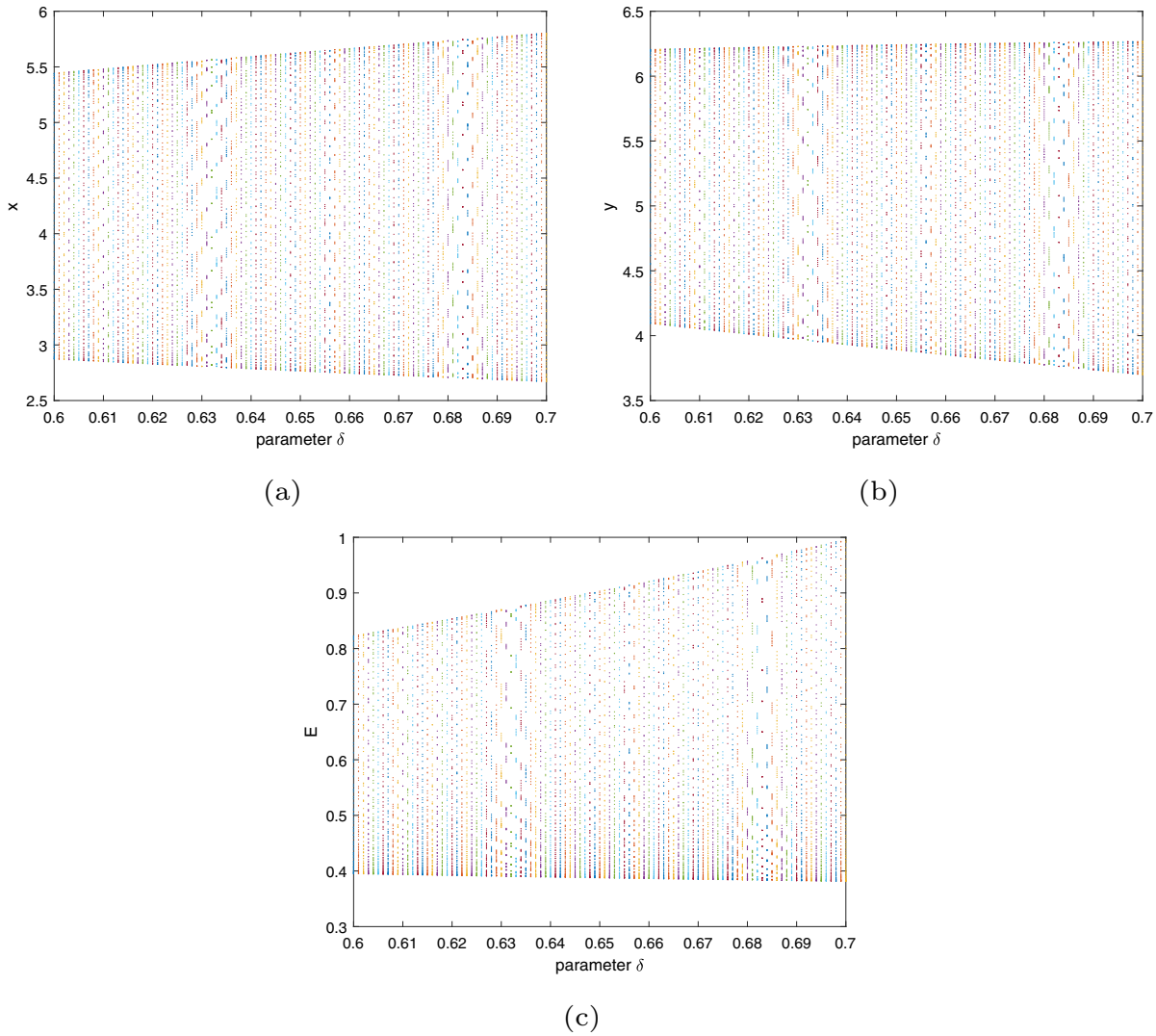

Fig. 5 The local amplification corresponding to Fig. 4a–c for δ in the range of 0.6 to 0.7

eter $\delta_1 = 0.504$. This phenomenon is further illustrated by the corresponding maximum Lyapunov exponent shown in Fig. 3. In addition, the phase space plots in Fig. 3a–e demonstrate the dynamics of $\delta \in (0.48, 0.58)$. Of particular note is the emergence of a chaotic ensemble at $\delta = 0.584854$, as shown in Fig. 3e. In Fig. 2, the maximum Lyapunov exponent corresponding to $\delta = 0.584854$ exceeds zero, thus verifying the existence of chaotic behavior. These simulations use the initial conditions $x(0) = 0.95$, $y(0) = 0.45$, and $E(0) = 0.3$ (Fig. 3).

In this example, we have uncovered the dynamic behaviors that may occur in complex systems. The system exhibits chaotic phenomena and the occurrence of trajectory bifurcations at intervals of 2, 4, and 8. Chaos manifesting as nonperiodicity and high complexity, while the occurrence of trajectory bifurcations at intervals of 2, 4, and 8 indicates distinct periodic behavior within the system. These phenomena remind us of the complexity and diversity of ecosystems, emphasizing the need for a more detailed study of dynamic changes within ecological systems. For biologists and ecologists, understanding these phenomena can help them better predict the behavior of ecosystems and optimize management and conservation strategies. Therefore, research on the chaotic behavior and the occurrence of trajectory bifurcations at intervals of 2, 4, and 8 of flip bifurcations is crucial for our understanding and maintenance of the stability and diversity of ecosystems.

Example 5.2 (**N–S bifurcation**) For the parameters $(r = 2, k = 8, t_h = 1, \upsilon = 2, \gamma = 1, q = 1, e = 3, c = 1, m_1 = 1, m_2 = 1, m = \frac{1}{4}, p = 1)$, which cover the range $(r, e, \gamma, \upsilon, t_h, k, c, p.q, m_1, m_2, m) \in \Xi_3$, Lemma 2

is verified by a simple computation that ensures the existence of the only positive immovable point of system (20). We take $X_0 = (4, 5.5, 0.5)$ as the initial point. After calculation, we found that a Neimark–Sacker bifurcation occurs at the stationary point $X_0 = (4, 5.5, 0.5)$, which occurs with a parameter value of $\delta_2 = 0.4090$ and an eigenvalue of $\lambda_\pm = 0.9744375 \pm 0.224632i$. At $\delta_2 = 0.4090$, the modulus of the eigenvalue $|\lambda_\pm| = 1, l = \frac{1}{16} > 0, \varsigma_0 = -9.6512 * 10^7 < 0$, and $\frac{\aleph_1^2}{\aleph_2} = 0.051136 \neq 2, 3$, a result that verifies the validity of Theorem 4.

By observing Fig. 4a–c, we can find that the fixed point $X_0 = (4, 5.5, 0.5)$ of system (20) demonstrates a stable state at $\delta < 0.4090$, an unstable state at the value of the Neimark–Sacker bifurcation parameter $\delta_2 = 0.4090$, and an unstable state at the value of the Neimark–Sacker bifurcation parameter $\delta_2 = 0.4090$, and when the δ exceeds 0.4090, an attractive invariant closed curve appears.

Figure 5 illustrates a localized zoom-in of Fig. 4a–c, where δ is in the range (0.6,0.7). Figure 6 illustrates the maximum Lyapunov exponent from Fig. 4, covering the range of δ (0.1,0.8). It is observed that within this range, some Lyapunov exponents are greater than 0 and some are less than 0, which suggests the existence of stable immobilized points or stable periodic windows within the chaotic region. According to the literature [30–32], positive Lyapunov exponents are considered to be characteristic of chaos.

Based on the corollary of Theorem 5 and Theorem 7, when $\delta = 0.38 < \delta_2 = 0.4090$, the positive fixed point of Eq. (20), $X_0 = (4, 5.5, 0.5)$, exhibits localized asymptotic stability. And when $\delta = 0.41 > \delta_2 = 0.4090$, an attraction-invariant closed curve emerges from $X_0 = (4, 5.5, 0.5)$. These inferences are supported by the computer simulations in Figs. 7 and 8, where the initial conditions of the simulations are set to $x(0) = 3.95, y(0) = 5.45, E(0) = 0.45$.

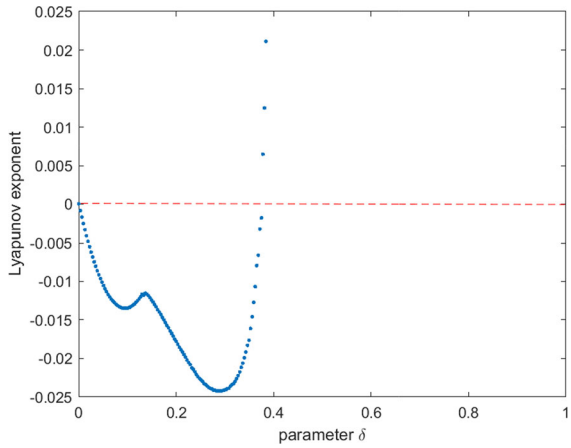

Fig. 6 The maximum Lyapunov exponents corresponding to Fig. 4a–c

8 Biological commentary

In this paper, we focus on stability and bifurcations in the predator–prey system with nonlinear prey harvesting and the square root functional response. Stability and bifurcations in the predator–prey system have important implications for ecology and biology, providing insights into understanding about the dynamics of interacting populations.

Biological significance of stability: In the model of this paper, according to simulation results and Theorem 5, when $\delta = 0.38 < \delta_2 = 0.4090$, the positive fixed point of Eq. (20), $X_0 = (4, 5.5, 0.5)$, exhibits localized asymptotic stability. A stable predator–prey system helps to maintain ecological balance and prevent drastic fluctuations in population size, thus protecting the ecosystem structure and function.

Biological significance of Flip bifurcation: In a predator–prey system, Flip bifurcation may lead to changes in the dynamic behavior between the predator and the prey. When the parameters change, the stable and periodic solutions between the predator and prey may alternate, thereby affecting the stability and dynamic balance of the ecosystem.The flip bifurcation has important biological implications in discrete predator–prey systems because it demonstrates the complex interactions between predators and prey. When predator populations reach critical thresholds, the system may undergo sudden state transitions from one stable state to another, which can lead to ecosystem collapse or transformation. This bifurcation phenomenon highlights the potential for abrupt change and instability in ecosystems, emphasizing the importance of predator–prey interactions for ecosystem structure and stability. Therefore, in-depth understanding and study of the flipping bifurcation phenomenon can help us better understand the dynamic properties of ecosystems and provide important insights for the conservation of biodiversity and effective management of ecosystems. In this article, we take δ as the bifurcation parameter. Through simulation, we demonstrate that when δ is increased to the limit value, the flip bifurcation occurs. We also elucidated the frequency of trajectory bifurcations in the intervals of 2, 4, and 8 and chaotic phenomena.

Biological significance of N–S bifurcation:The Neimark–Sacker phenomenon tells us that system responses to parameter changes create stable and unstable regions in parameter space. Understanding these regions is critical for us to predict and manage ecosystem responses. By studying the N–S bifurcation, biologists and ecologists can figure out the stability and dynamic behavior of ecosystems under different parameter conditions, which provides us with guidance for conserving and managing ecosystems. In addition, the N–S bifurcation provides a framework for understanding the interactions between stability and instability in ecosystems, helping us to better understand ecosystem stability and resilience. In this paper, we take δ as the bifurcation parameter. Through simulation, we demonstrate that when δ is increased to the limit value, the N–S bifurcation occurs.

Overall, the study of stability and bifurcations in predator–prey systems provides profound ecological insights into under-

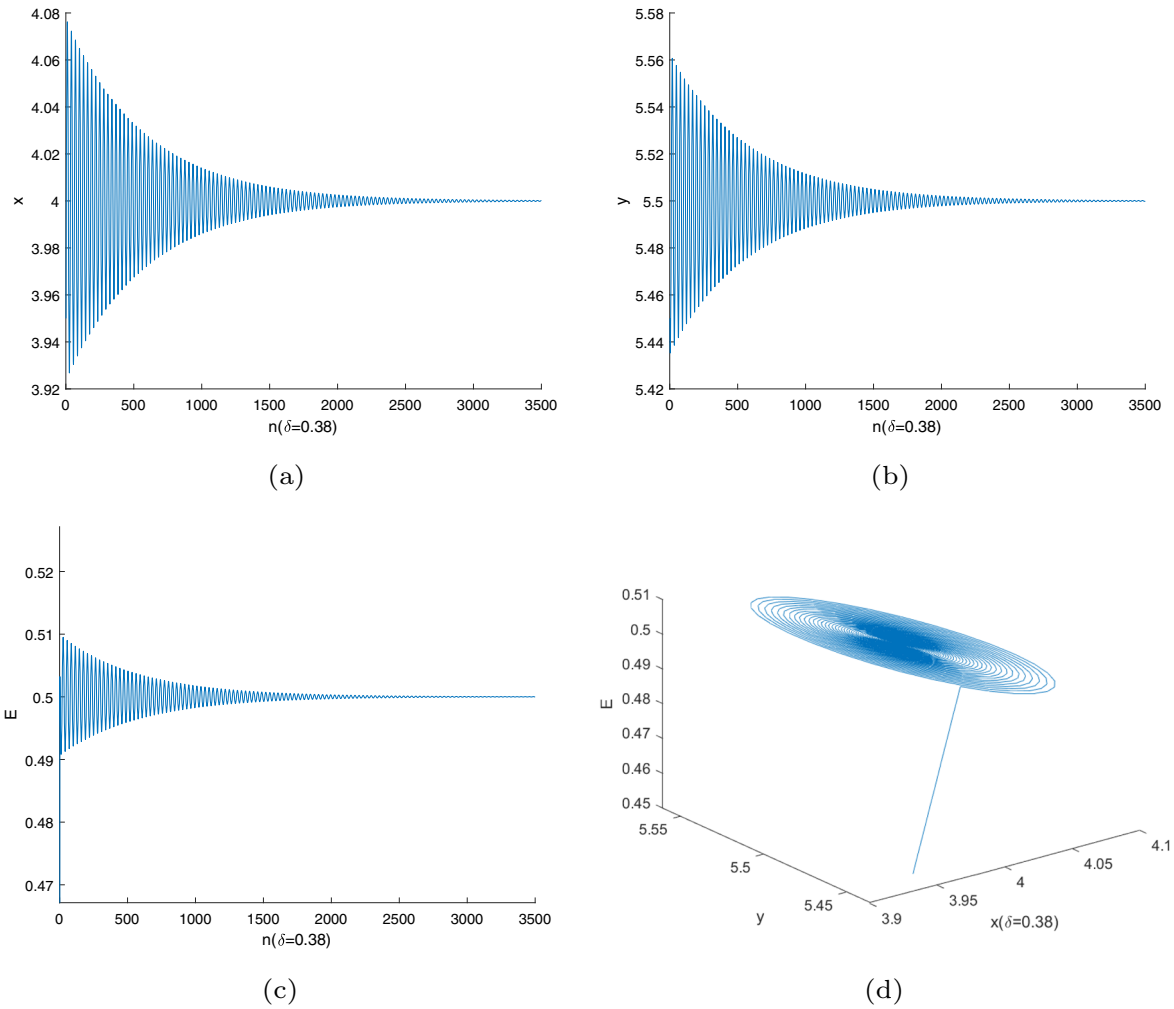

Fig. 7 When $\delta = 0.38$, which is less than the critical value $\delta_2 = 0.4090$, the fixed point (4, 5.5, 0.5) in case (ii) exhibits stability. The initial values are set at (3.95, 5.45, 0.45)

standing how biological systems adapt and respond to environmental change. The understanding of these concepts has broad applications for fields such as ecology, conservation biology, and sustainable resource management.

9 Discussion

In our study, we mainly analyze a novel discrete differential-algebraic bioeconomic system with flip and Neimark–Sacker bifurcation. Our study finds that for different step sizes δ, the fixed point of the system (20) may be destabilized by either flipping or Neimark–Sacker bifurcation accompanied by a positive Lyapunov exponent, indicating the presence of chaotic phenomena.

Our results extend previous studies, especially with respect to [33], by demonstrating richer and more intriguing dynamical behaviors in discrete models.

In addition, this paper introduces a novel and effective method for analyzing chaos and bifurcation phenomena in more complex discrete differential-algebraic systems. These findings set the stage for future research on similar topics.

During the process of writing the paper, we encountered the following problems and challenges: the simulation model contains many parameters that need to be estimated. Determining accurate parameter values may require multiple experiments and adjustments, increasing the complexity and time consumption of the simulation process.

In the future, we can study discrete predator–prey systems from the following perspectives:

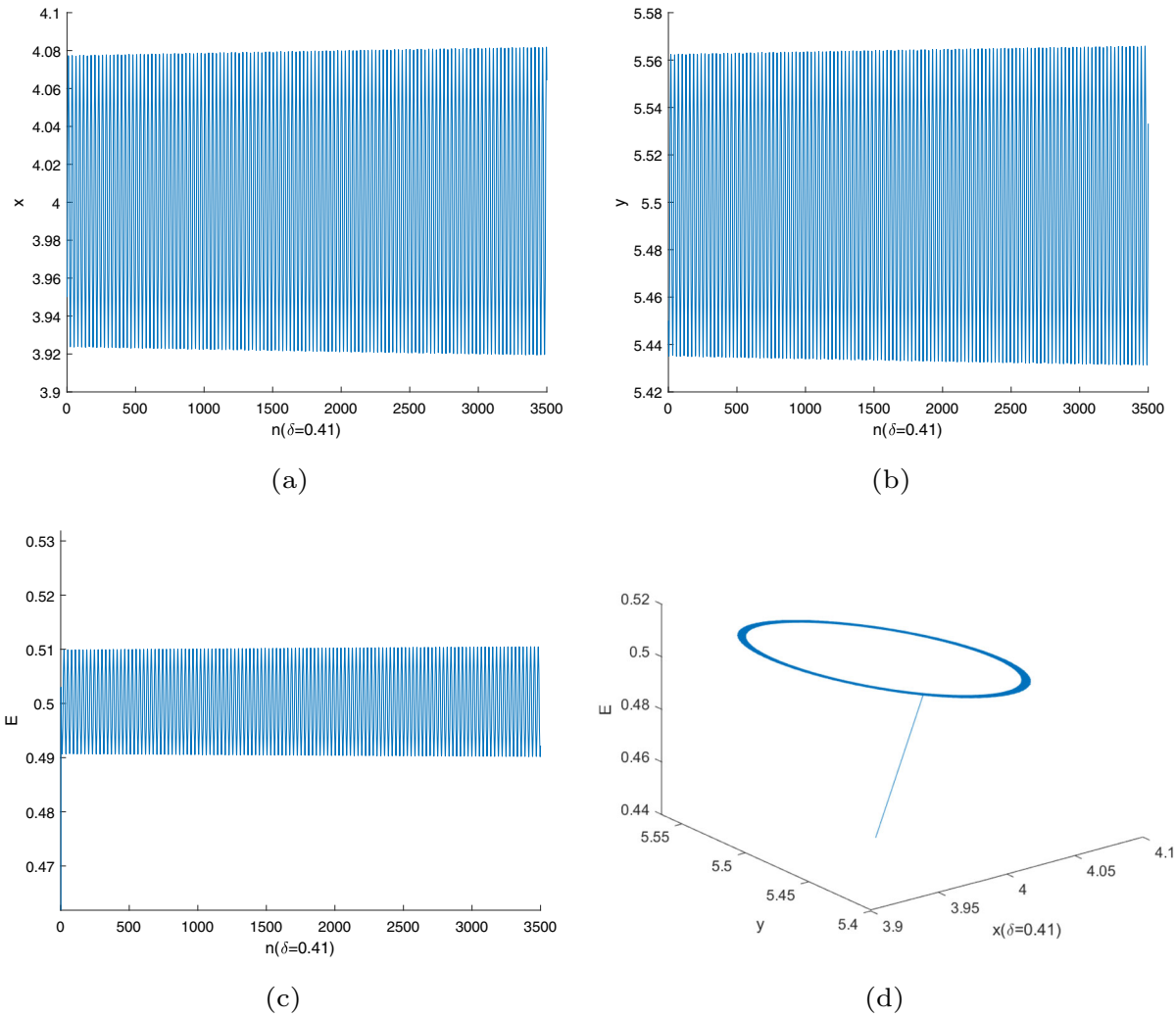

Fig. 8 When $\delta = 0.41$, surpassing the critical value $\delta_2 = 0.4090$, an attracting invariant closed curve emerges from the stable fixed point (4, 5.5, 0.5) in case (ii). The initial values are specified as (3.95, 5.45, 0.45)

We can adopt more complex and refined mathematical models to more comprehensively reveal the dynamic behavior of discrete predator–prey systems. These models can consider more influencing factors, such as environmental changes, competition between predators and prey, population migration and diffusion, etc. By using these more detailed models, we can simulate various complex dynamic phenomena in the system, such as periodic population fluctuations, spatial distribution patterns of populations, and interactions between different populations in the ecosystem.

We can further study the effect of system parameters on ecosystem stability, such as predator and prey population size and environmental changes, among other factors. This will help us to predict the stability of the ecosystem and develop more effective ecological management strategies.

We can explore coupled systems and multiple population interactions. Considering the interactions between different populations in an ecosystem, future studies could couple discrete predator–prey systems with other biological populations or environmental factors to gain a more comprehensive understanding of ecosystem dynamics.

We can conduct field observations and experiments to validate the models in the future, and use the results of the research in practical ecosystem management and conservation, which is crucial for promoting sustainable development and conservation of the ecosystem.

We can model and predict discrete predator–prey systems in the future by using data and machine learning techniques, and we can more accurately understand ecosystem changes and

develop more effective management and conservation strategies.

Finally, we can also use more advanced numerical simulation methods and computational techniques to more accurately analyze and predict the stability and dynamic behavior of the system. By conducting large-scale parameter scanning and sensitivity analysis on the model, we can discover the key parameters in the system and their impact on system behavior. This will help us better understand the stability mechanism of the system and provide theoretical support for developing more effective ecological management strategies.

Acknowledgements This work is supported by the National Science Foundation of China under Grant Nos. 61976228 and 62076229, the Fundamental Research Funds of South-Central Minzu University (CZQ24020).

Author contributions H.G. and G.Z. wrote the main manuscript text and L.W. prepared some data. All authors reviewed the manuscript.

Data availability No datasets were generated or analysed during the current study.

Declarations

Conflict of interest The author(s) declare no potential conflicts of interest with respect to the research, authorship, and/or publication of this article.

References

1. Luo, J., Zhao, Y.: Stability and bifurcation analysis in a predator–prey system with constant harvesting and prey group defense. Int. J. Bifurc. Chaos **27**(11), 1750179 (2017)
2. Dou, R., Wang, C.: Bifurcation analysis of a predator–prey model with memory-based diffusion. Nonlinear Anal. Real World Appl. **75**, 103987 (2024). https://doi.org/10.1016/j.nonrwa.2023.103987
3. Zhou, G., Ma, L., Wang, Y.: Population dynamics in a reaction–diffusion–advection predator-prey model with Beddington–DeAngelis functional response. Nonlinear Anal. Real World Appl. **77**, 104059 (2024). https://doi.org/10.1016/j.nonrwa.2023.104059
4. Qurban, M., Khaliq, A., Saqib, M., Abdeljawad, T.: Stability, bifurcation, and control: modeling interaction of the predator–prey system with Alles effect. Ain Shams Eng. J. (2024). https://doi.org/10.1016/j.asej.2024.102631
5. Zhou, J.: Bifurcation analysis of a diffusive predator-prey model with ratio-dependent holling type iii functional response. Nonlinear Dyn. **81**(3), 1535–1552 (2015)
6. Shi, Q., Song, Y.: Spatially nonhomogeneous periodic patterns in a delayed predator–prey model with predator-taxis diffusion. Appl. Math. Lett. **131**, 108062 (2022)
7. Xu, C., Zhang, W., Aouiti, C., Liu, Z., Yao, L.: Bifurcation insight for a fractional-order stage-structured predator–prey system incorporating mixed time delays. Math. Methods Appl. Sci. **46**(8), 9103–9118 (2023)
8. Zhang, G., Shen, Y., Chen, B.: Positive periodic solutions in a non-selective harvesting predator-prey model with multiple delays. J. Math. Anal. Appl. **395**(1), 298–306 (2012)
9. Ghosh, B., Barman, B., Saha, M.: Multiple dynamics in a delayed predator-prey model with asymmetric functional and numerical responses. Math. Methods Appl. Sci. **46**(5), 5187–5207 (2023)
10. Santra, N., Saha, S., Samanta, G.: Role of multiple time delays on a stage-structured predator–prey system in a toxic environment. Math. Comput. Simul. **212**, 548–583 (2023)
11. Du, W., Xiao, M., Ding, J., Yao, Y., Wang, Z., Yang, X.: Fractional-order PD control at hopf bifurcation in a delayed predator-prey system with trans-species infectious diseases. Math. Comput. Simul. **205**, 414–438 (2023)
12. Liang, Z., Meng, X.: Stability and hopf bifurcation of a multiple delayed predator-prey system with fear effect, prey refuge and Crowley–Martin function. Chaos Solitons Fractals **175**, 113955 (2023)
13. Xu, C., Mu, D., Pan, Y., Aouiti, C., Yao, L.: Exploring bifurcation in a fractional-order predator–prey system with mixed delays. J. Appl. Anal. Comput **13**, 1119–1136 (2023)
14. Barman, B., Ghosh, B.: Role of time delay and harvesting in some predator–prey communities with different functional responses and intra-species competition. Int. J. Model. Simul. **42**(6), 883–901 (2022)
15. Jiao, X., Li, X., Yang, Y.: Dynamics and bifurcations of a Filippov Leslie-Gower predator–prey model with group defense and time delay. Chaos Solitons Fractals **162**, 112436 (2022)
16. Wang, C., Li, X.: Further investigations into the stability and bifurcation of a discrete predator–prey model. J. Math. Anal. Appl. **422**(2), 920–939 (2015)
17. Pal, A.K.: Controlling chaotic dynamics of a delayed Hassell-Varley type predator–prey model with non-linear harvesting efforts in prey by using imprecise biological parameters. Results Control Optim. **14**, 100361 (2024). https://doi.org/10.1016/j.rico.2023.100361
18. Bhunia, B., Ghorai, S., Kar, T.K., Biswas, S., Bhutia, L.T., Debnath, P.: A study of a spatiotemporal delayed predator-prey model with prey harvesting: constant and periodic diffusion. Chaos Solitons Fractals **175**, 113967 (2023)
19. Upadhyay, R.K., Agrawal, R.: Dynamics and responses of a predator–prey system with competitive interference and time delay. Nonlinear Dyn. **83**(1–2), 821–837 (2016)
20. Wang, Y., Zou, X.: On a predator–prey system with digestion delay and anti-predation strategy. J. Nonlinear Sci. **30**(4), 1579–1605 (2020)
21. Owolabi, K.M., Pindza, E., Karaagac, B., Oguz, G.: Laplace transform-homotopy perturbation method for fractional time diffusive predator–prey models in ecology. Partial Differ. Equ. Appl. Math. **9**, 100607 (2024). https://doi.org/10.1016/j.padiff.2023.100607
22. Yin, W., Li, Z., Chen, F., He, M.: Modeling Allee effect in the Leslie-Gower predator-prey system incorporating a prey refuge. Int. J. Bifurc. Chaos **32**(06), 2250086 (2022)
23. Bi, Z., Liu, S., Ouyang, M., Wu, X.: Pattern dynamics analysis of spatial fractional predator–prey system with fear factor and refuge. Nonlinear Dyn. (2023)
24. Zhang, G., Shen, Y., Chen, B.: Bifurcation analysis in a discrete differential-algebraic predator-prey system. Appl.

Math. Model. **38**(19), 4835–4848 (2014). https://doi.org/10.1016/j.apm.2014.03.042
25. Din, Q.: Complexity and chaos control in a discrete-time prey–predator model. Commun. Nonlinear Sci. Numer. Simul. **49**, 113–134 (2017). https://doi.org/10.1016/j.cnsns.2017.01.025
26. Uddin, M.J., Rana, S.M.S., Işık, S., Kangalgil, F.: On the qualitative study of a discrete fractional order prey–predator model with the effects of harvesting on predator population. Chaos Solitons Fractals **175**, 113932 (2023). https://doi.org/10.1016/j.chaos.2023.113932
27. Mortuja, M.G., Chaube, M.K., Kumar, S.: Dynamic analysis of a predator–prey system with nonlinear prey harvesting and square root functional response. Chaos Solitons Fractals **148**, 111071 (2021)
28. Gordon, H.S.: The economic theory of a common-property resource: the fishery. J. Polit. Econ. **62**(2), 124–142 (1954)
29. Chen, B., Liao, X., Liu, Y.: Normal forms and bifurcations for the differential-algebraic systems. Acta Math. Appl. Sin. **23**(3), 429–443 (2000)
30. Wiggins, S.: Chaos and strange attractors. Introduction to Applied Nonlinear Dynamical Systems and Chaos, pp. 736–746 (2003)
31. Carr, J.: Applications of Center Manifold Theory. Springer, Berlin (1981)
32. Guckenheimer, J., Holmes, P.: Nonlinear Oscillations, Dynamical Systems and Bifurcations of Vector Fields. Springer, New York (1983)
33. Guo, H., Han, J., Zhang, G.: Hopf bifurcation and control for the bioeconomic predator–prey model with square root functional response and nonlinear prey harvesting. Mathematics **11**(24), 4958 (2023)
34. Zhang, G., Zhu, L., Chen, B.: Hopf bifurcation in a delayed differential-algebraic biological economic system. Nonlinear Anal. Real World Appl. **12**(3), 1708–1719 (2011)
35. Zhang, G., Zhu, L., Chen, B.: Hopf bifurcation and stability for a differential-algebraic biological economic system. Appl. Math. Comput. **217**(1), 330–338 (2010). https://doi.org/10.1016/j.amc.2010.05.065
36. Liu, X., Liu, P., Liu, Y.: The existence of codimension-two bifurcations in a discrete-time sir epidemic model. AIMS Math. **7**(3), 3360–3379 (2022)
37. Khan, A.Q., Akhtar, T., Jhangeer, A., Riaz, M.B.: Codimension-two bifurcation analysis at an endemic equilibrium state of a discrete epidemic model. AIMS Math. **9**(5), 13006–13027 (2024)
38. Zhang, G., Shen, Y., Chen, B.: Hopf bifurcation of a predator–prey system with predator harvesting and two delays. Nonlinear Dyn. **73**(4), 2119–2131 (2013)
39. Liu, X., Xiao, D.: Complex dynamic behaviors of a discrete-time predator-prey system. Chaos Solitons Fractals **32**(1), 80–94 (2007)
40. Kuznetsov, Y.A., Kuznetsov, Y.A.: Numerical analysis of bifurcations. Elements of applied bifurcation theory, pp. 505–585 (2004)
41. Liu, X., Liu, Y.: Codimension-two bifurcation analysis on a discrete Gierer-Meinhardt system. Int. J. Bifurc. Chaos **30**(16), 2050251 (2020)
42. Wu, X.P., Wang, L.: Analysis of oscillatory patterns of a discrete-time Rosenzweig-Macarthur model. Int. J. Bifurc. Chaos **28**(06), 1850075 (2018)

Publisher's Note Springer Nature remains neutral with regard to jurisdictional claims in published maps and institutional affiliations.

Springer Nature or its licensor (e.g. a society or other partner) holds exclusive rights to this article under a publishing agreement with the author(s) or other rightsholder(s); author self-archiving of the accepted manuscript version of this article is solely governed by the terms of such publishing agreement and applicable law.